Combinatorial Approaches to Controlling Cell Behaviour and Tissue Formation in 3D *via* Rapid-Prototyping and Smart Scaffold Design

Tim B.F. Woodfield[*,1,2], Lorenzo Moroni[3] and Jos Malda[4]

[1]*Department of Orthopaedic Surgery, University of Otago Christchurch, Christchurch, New Zealand*

[2]*Centre for Bioengineering, University of Canterbury, Christchurch, New Zealand*

[3]*Department of Biomedical Engineering, Johns Hopkins University, Baltimore MD, USA*

[4]*Department of Orthopaedics, University Medical Centre Utrecht, The Netherlands*

Abstract: The understanding of fundamental phenomena involved in tissue engineering and regenerative medicine is continuously growing and leads to the demand for three-dimensional (3D) models that better represent tissue architecture and direct cells into the proper lineage for specific tissue repair. Porous 3D scaffolds are used in tissue engineering as templates to allow cell attachment and tissue formation. Scaffold design plays a central role in guiding cells to synthesize and maintain new tissues. While a number of techniques have been developed and are now in use for high-throughput screening of combinatorial factors involved in biotechnology in two-dimensions, high-throughput screening in 3D is still in its infancy. There is a broad interest in developing similar techniques to assess which variables are critical in designing 3D scaffolds to achieve proper and lasting tissue regeneration. We describe, herein, a number of studies adopting smart scaffold design and *in vitro* and *in vivo* analysis as the basis for 3D model systems for evaluating combinatorial factors influencing cell differentiation and tissue formation.

1. INTRODUCTION

Many new combinatorial and high-throughput methods for screening cell response to biomaterials have been developed recently [1-14]. With the recent exponential growth in the fields of tissue engineering and regenerative medicine [15], numerous scaffold materials and designs have been described in literature related to the repair or regeneration of damaged human tissues [16-21]. For example, the treatment of damage to articulating joints, such as the knee or hip, is a challenge for orthopaedic surgeons world-wide. It is well established that the layer of articular cartilage covering the surface of articulating joints has limited regenerative capacity, and that these lesions are a major cause of pain, swelling, and mechanical impairment. In addition, if left untreated, damage to the articular cartilage may lead to osteoarthritis (OA), causing considerable disability and limitations to activities of daily living.

Tissue engineering and regenerative medicine strategies hold promise for the treatment of damaged cartilage by the delivery of cells and/or bioactive factors *via* three-dimensional (3D) biodegradable scaffold conduits. However, the majority of these approaches have not addressed the high degree of topographical organisation of cells and extracellular matrix (ECM) constituents within native tissues. Tissue engineering solutions will likely require the combination of a number of complex cell and material interactions to achieve a satisfactory result *in vivo*. Porous scaffolds play a central role in controlling a number of these factors. For example, they provide (i) a delivery vehicle (*ex vivo*) or recruitment vehicle (*in vivo*) for cells or growth factors, (ii), a porous 3D environment for production of ECM as well as nutrient and waste exchange, and (iii) mechanical properties to match those of the surrounding host tissues.

While considerable progress has been made, the lamentable reality is that tissue engineering of functional tissue of clinically relevant size still remains largely elusive [16-18, 22, 23]. If successful repair or replacement requires grown tissue possessing the functional properties of the native tissue [16, 24], then it appears that we are still very much in the infancy stage of the generally accepted tissue-engineering paradigm [25, 26]. Without a clear understanding and characterisation of the influence of the biomaterial and scaffold architecture on cellular function in 3D (discussed later in Section 2), it is often impossible to make comparisons between studies using various scaffolds, as well as make clear distinctions as to which scaffold characteristics are responsible for eliciting observed *in vitro* and/or *in vivo* responses without time consuming trial and error approaches.

Combinatorial and high-throughput screening approaches may help accelerate discovery and reduce the complexity associated with characterizing new biomaterials for tissue engineering and regenerative medicine applications [6, 8, 27]. The ability to elucidate how the abovementioned factors influence cell re-differentiation and formation of functional 3D tissues both on an individual and collective basis requires the use of smart scaffold design in combination with *in vitro* and *in vivo* analysis to develop model systems or high-throughput screening tools for tissue engineering. Many studies that screen the *in vitro* or *in vivo* performance and biocompatibility of biomaterials and/or surface modifications adopt 2D models, such as films or substrates. However,

*Address correspondence to this author at the Department of Orthopaedic Surgery, University of Otago, Christchurch, P.O. Box 4345, Christchurch 8140, New Zealand; Tel: +64 3 364-1086; Fax: +64 3 364-0909;
E-mail: tim.woodfield@otago.ac.nz

1386-2073/09 $55.00+.00

tissues are complex 3D structures, and cell behaviours observed in 2D [28-32] are not always reflected in 3D [33-36]. Due to these increasingly recognised limitations of 2D models, it is important to consider this additional dimension and establish rigorous screening methods for extended studies in 3D scaffolds [6, 37].

Current approaches to screening the influence of various media components, growth factors or cell types on cell differentiation and tissue formation includes micro-mass (or pellet) culture [38-41] as well as filter differentiation (or hanging drop) cultures [42]. While 3D tissue formation can be evaluated to a degree, as cells coalesce into spherical pellets, the process is man-power intensive, requiring individual tubes or wells for each pellet. More importantly, there is no capacity for evaluating cell-biomaterial interactions and their small size (i.e. <Ø2mm) means that pellet culture models do not accurately represent tissue engineering strategies or the clinical setting, where large volumes of tissue (i.e. cm^3 of bone or articular cartilage) are necessary, thereby introducing constraints based on high cell numbers required and nutrient diffusion throughout large tissue constructs.

One of the challenges in tissue engineering is the design and fabrication of biodegradable scaffolds that can direct and regulate specific cellular functions, such as cell adhesion, proliferation, specific phenotypic expression and ECM deposition in a predictable and controlled fashion. Taking the example of articular cartilage and cartilage tissue engineering strategies, it is well established that chondrocytes require a 3D environment to maintain their differentiated phenotype [16, 43-46] and synthesize ECM components, such as collagen type II and glycosaminoglycan (GAG), which in turn provide the tissue with its impressive biomechanical properties [47, 48]. Little is known, however, about the specific influence of controlled changes in 3D scaffold architecture on chondrocyte (re)differentiation. It has been suggested that scaffold architecture may control cell function by regulating the diffusion of nutrients (e.g., oxygen, glucose) and waste products, as well as influencing cell-cell interactions [49].

Among the scaffold-based approaches commonly used for cartilage and other tissue engineering applications, hydrogels offer a broad selection to provide a controlled 3D milieu for cells, thereby representing a promising class of scaffolds for improving cell-cell signalling, tissue formation and integration [50-54]. Different cell sources have been readily encapsulated in synthetic or natural hydrogels and showed to support regeneration of various tissues [55-60]. Furthermore, hydrogels can be also modified or functionalised with a number of different peptides [6, 59, 61-65] and proteins [66-68] to enhance cell-biomaterial interactions when needed. Recent studies have also demonstrated the capability of multi-layered hydrogels to function as models to study cell-cell interactions and the resulting implications in tissue formation [58, 69]. In this respect, more studies adopting hydrogels should be considered as possible scaffold platforms for high-throughput screening of cell-cell and cell-biomaterials interactions in three-dimensions. However, poor mechanical properties [70, 71] and nutrient diffusion limitations for large tissue-engineered constructs [72] may pose some limits to their use for soft tissue applications. Although a possible solution to nutrient limitations may be offered by creating a larger and more accessible pore network through the use of porogens or by processing these biomaterials with rapid prototyping technologies [73-75], enhanced mechanical properties are still a challenge.

With respect to the design and characterisation of specific scaffold architectures, pore interconnectivity is an important factor and is often overlooked. A scaffold may contain pores making it porous, but unless the pores are interconnected (*i.e.* voids linking one pore to another), they hinder cell infiltration and tissue formation and serve no purpose in a scaffold for tissue engineering. The size of interconnections between pores should be suitably large to support ECM infiltration and vascularisation of the desired tissue and, therefore, considerations for pore interconnectivity are often more critical than pore size. It is preferable that scaffolds designed for tissue engineering strategies have 100% interconnecting pore volume (i.e. the entire pore volume can be accessed from the periphery to the centre and vice versa), thereby also maximizing the diffusion and exchange of nutrients throughout [37, 76, 77].

With any approach to biomaterial or scaffold design, the specific model adopted for screening cell behaviour and tissue formation *in vitro* or *in vivo* will depend ultimately on the material under investigation, and the unique set of criteria required to meet the specific clinical application, such as: the cell type and source; control of cell adhesion, proliferation and differentiation, as well as biomaterial processing, composition, degradation rate and pore architecture. The controlled design of 3D scaffolds should allow selection of (i) pore size, (ii) biomaterial composition, (iii) pore architecture/geometry, (iv) bulk scaffold shape (simple or complex from CT/MRI images), and (v) pore interconnectivity [16, 46, 78]. We can take advantage of these scaffold design criteria to develop 3D model systems to systematically study or screen the following: (i) scaffold mechanical properties, (ii) effects of biomaterial composition on tissue formation, (iii) effects of pore architecture/geometry on tissue formation, and (iv) the effects of pore architecture/geometry on nutrient diffusion.

In this article, we discuss a series of experiments and model systems developed by the authors to evaluate chondrocyte (re)differentiation and articular cartilage tissue engineering strategies with respect to controlled scaffold 3D pore architecture, scaffold pore-size gradients, single- or multiphasic scaffold compositions, growth factor release, and the measurement and modelling of mechanical properties and nutrient gradients. Furthermore, we discuss the basis for adopting smart scaffold design to evaluate combinatorial factors influencing cell differentiation and tissue formation in 3D.

There are many ways to producing "smart scaffolds" for controlling cell-biomaterial interactions e.g., surface modification, functionalised hydrogels, self-assembling peptides, incorporation of RGD sequences and/or growth factors to name a few. Our combinatorial approach to developing designed scaffolds in terms of optimising architecture, composition and mechanical properties to control cell distribution and "instruct" differentiation is a departure from what would more conventionally be termed a "smart scaffold". However, we stress that "smart scaffolds" also result from "smart scaffold design". The premise behind these studies is the question of what a cell "sees" in 2D versus 3D environments, and

what the implications are for designing smart methods for controlling cell behaviour, and ultimately tissue function.

2. ADVANCED SCAFFOLD DESIGN AND FABRICATION VIA RAPID PROTOTYPING

One of the major advances in understanding how 3D scaffold design can influence cell and tissue behaviour has been the ability to take control of fabricating porosity into biomaterials. Numerous processing techniques have been developed to produce porous biomaterial scaffolds for tissue engineering applications. By far the most common techniques for generating porosity include the various forms of foaming, particle leaching, and woven/non-woven fibre meshes or textiles [79-84]. While the size and distribution of pores can be controlled to a degree, the position and orientation of these pores is inherently random. The control over scaffold architecture using these conventional fabrication techniques are highly "process" driven rather than "design" driven. This lack of control in pore structure, particularly with respect to the interconnectivity between pores, makes it difficult to systematically screen biomaterials or compare scaffold architectures with another. In these instances, there are often unavoidable random components inherent to the pore architecture or composition of each sample which could influence the quality and quantity of tissue formed, such as: cell content; cell adhesion, proliferation and migration; cell differentiation; nutrient supply; mechanical properties and biodegradation rate.

As a result, investigators have recently turned to rapid prototyping (RP) or solid free-form fabrication (SFF) techniques for producing porous scaffolds for tissue engineering applications [75, 78, 85-91]. RP encompasses a range of processing techniques which allow highly complex and reproducible structures to be constructed one layer at a time *via* computer-aided design (CAD) models and computer-aided machining (CAM) or robotic handling. These techniques essentially allow researchers to design-in desired properties, such as porosity, interconnectivity and pore size, in a number of polymer and ceramic materials [87, 92-96]. Application of this technology in combination with modern clinical imaging techniques, such as computed tomography (CT) and magnetic resonance imaging (MRI), has resulted in recent advances in producing customized porous scaffolds for tissue engineering [88, 92, 96, 97].

The predominant RP platform adopted for studies described herein for developing model scaffold architectures was 3D Plotting, also named as 3D fibre deposition (3DF). 3DF scaffolds were produced using a computer controlled X-Y-Z plotting device (Bioplotter, Envisiontec GmbH, Germany) that has been extensively described [16, 37, 77, 98-106]. Additional modifications to the device enable the extrusion of highly viscous polymer melts (Fig. **1**), thereby providing a flexible fabrication platform to incorporate a large range of scaffold parameters and biomaterial compositions.

Briefly, bio-polymer granules are placed in a stainless steel syringe and heated at 190-220°C *via* a thermostatically controlled cartridge unit, fixed to the "X"- arm of the device. When the polymer reaches a molten phase, a nitrogen pressure (4-5 bar) is applied to the syringe through a pressurized cap. CAD models (i.e. simple blocks or complex shapes based on anatomical CT or MRI data) are then loaded into the Bioplotter CAM software and corresponding scaffolds deposited in a layer-by-layer process, through the extrusion of rapidly solidifying polymer fibres onto the X-Y stage (Fig. **1**). Heating temperature and extrusion pressure can be altered depending on the viscosity of the polymer composition processed. Scaffolds are then rendered by varying the fibre diameter (through the nozzle diameter), the spacing between fibres in the same layer, the layer thickness, and the angle of orientation of the deposited fibres (e.g., 0–45 and 0–90 configurations). The architecture could be changed by modifying the fibre orientation after one or two deposited layers (referred to as single and double layer configurations), as depicted in Fig. (**1a**, **b**) respectively. The deposition speed could also be varied (100-300 mm/min), to further control both the fibre diameter and the overall porosity of the scaffolds. The variation of each of these parameters singularly or in combination allows fabrication of a wide range of 3D scaffolds with controlled pore volume and shape. This makes 3DF and RP technologies appealing platforms to screen both

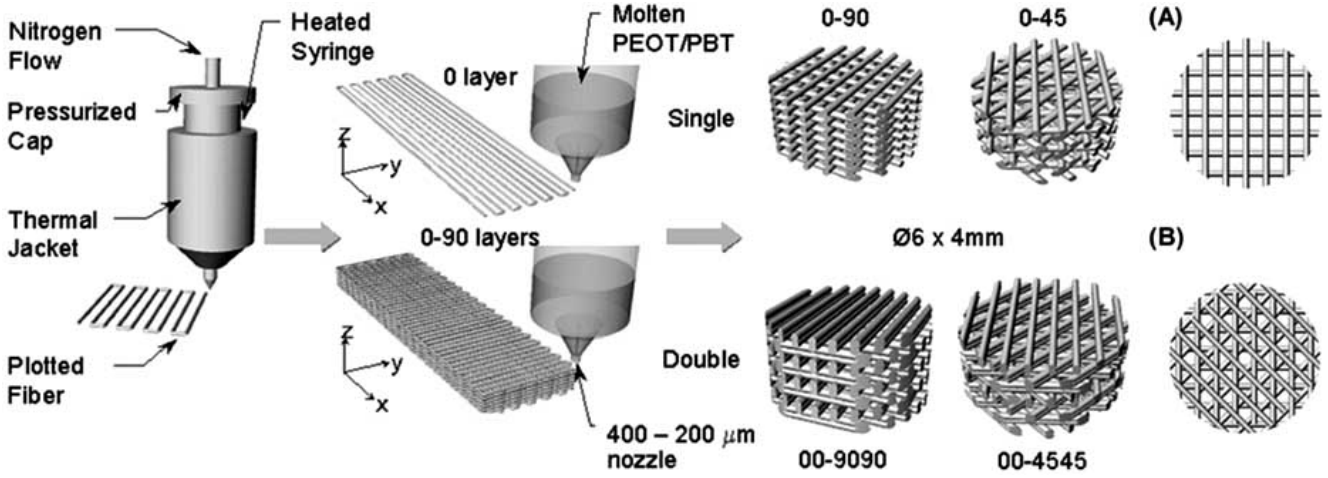

Fig. (1). Illustration of the 3D Plotting or 3DF fabrication process. Scaffold architectures (0–90 and 0–45) in single and double layer versions are illustrated demonstrating (**A**) quadrangular and (**B**) polygonal pore shapes. (Reprinted from Moroni *et al*. [103] with permission).

scaffolds and the dynamics of tissue formation in 3D.

As a model substrate for designing scaffolds and investigating cell-biomaterial relationships for tissue engineering, we evaluated a series of amphiphilic, biodegradable poly(ether ester) block co-polymers based on hydrophilic poly(ethylene glycol)-terephthalate (PEGT) and hydrophobic poly(butylene terephthalate) (PBT) blocks. The composition is denoted as *a*/*b*/*c*, where *a* represents the poly(ethylene glycol) (PEG) molecular weight (MW g/mol), and *b* and *c* represent the weight percentage (wt%) of PEGT and PBT blocks respectively. Due to a variable degree of substitution and MW of PEG during co-polymerization [83], these co-polymers can also be termed as PEOT/PBT.

A major advantage of these types of co-polymer systems is that, by varying the PEG MW and the weight percentage of hydrophilic PEGT and hydrophobic PBT blocks, an entire family of polymers could be obtained. This offered extensive possibilities in the design of model co-polymer systems with tailor-made properties, such as wettability [107], protein adsorption [108], swelling [109], biodegradation rate [109], and mechanical properties [100, 103, 105]. Being polyether-esters, degradation occurs in aqueous media, by hydrolysis and oxidation, at a rate that varies from months to years. High PBT contents result in slow degradation rates whereas higher PEGT content and PEG MW results in more rapid degradation [109-111]. Furthermore, the addition of 0.2 wt% α-tocopherol as an antioxidant provides stability to the PEGT/PBT co-polymers at elevated temperatures, thus providing suitable viscosities to support a wide range of processing techniques [100] such as 3DF.

Various *in vitro* and *in vivo* studies have demonstrated both the biocompatibility and biodegradable nature of PEGT/PBT co-polymers [109, 112-114] with 1000/70/30, 1000/60/40 and 300/55/45 compositions evaluated for a range of biomedical applications, including tissue engineering of bone and skin [83, 109, 112, 115-120]. Protein adsorption as well as the attachment, proliferation, morphology, and differentiation state of chondrocytes has been demonstrated on different compositions of 2D PEGT/PBT films [32, 108, 121, 122] as has articular cartilage tissue formation on a range of porous 3D PEGT/PBT scaffolds [16, 37, 77, 98-102, 104, 123]. Controlled release of bioactive factors from these materials has also been demonstrated [16, 124].

3. THE EFFECT OF 3D PORE ARCHITECTURE ON MEASUREMENT AND MODELLING OF DYNAMIC MECHANICAL PROPERTIES OF SCAFFOLDS

As introduced earlier, RP and SFF platforms allow tailoring of scaffold architecture. In this respect, 3DF could be an appealing tool to screen the influence of scaffold fabrication parameters on its mechanical and physicochemical properties, and on the tissue formation capacities of the resulting templates. Two possible strategies can be followed to regenerate a natural tissue in a scaffold-based tissue engineering approach: (i) fabricating scaffolds with mechanical properties matching those of the desired repair tissue; or (ii) optimizing scaffolds' phyisicochemical properties and porosity to favour a proper cell-material interaction and cell ingrowth. Whereas the latter strategy allows enhanced tissue formation, constructs have to be cultured *in vitro* for long periods (months *vs* days) to achieve adequate mechanical properties for implantation. This often results in a laborious and expensive process. Therefore, the former approach is typically preferred as a requirement for scaffold design and fabrication, since it allows early *in vivo* implantation of tissue-engineered constructs. Mechanical properties of 3D scaffolds can be appropriately modulated through novel fabrication techniques like SFF, by varying scaffold pore size and shape. As previously mentioned, these scaffolds display completely interconnected pores and can be fabricated with a wide range of biomaterials. Therefore, 3D constructs with optimized initial mechanical, physicochemical, and structural properties can be produced by SFF for specific demands.

In particular, this set of fabrication technologies is characterized by a precise control over the manufacturing parameters, resulting in scaffolds with a periodical pore network and architecture. A change in pore size results in a variation of the scaffold's porosity and in a consequent modification of its mechanical properties [103, 105]. Specifically, an increase in porosity would produce a decrease in the elastic response of the scaffolds measured as equilibrium modulus and/or dynamic stiffness. Analogously, scaffolds with different pore shape and same porosity possess different mechanical properties, as the number of contact points between the struts of a pore - generally fibers - varies [105]. Hence, if pore architecture is superimposed on scaffold porosity, mechanical properties can be modulated by either varying pore shape and/or size. This modulation could be mathematically modeled due to the periodicity of SFF scaffolds. A recent study showed that the dynamic stiffness of SFF scaffolds could be modulated with different pore size and architecture to match the dynamic stiffness of articular and meniscal cartilage [103]. The dynamic stiffness of these constructs followed an exponential decay with increasing porosity, which was strictly dependent on the chosen pore architecture. In particular the dynamic stiffness E' was found to vary as:

$$E' = E_0 \cdot e^{-\alpha \cdot P} \quad (1)$$

where, E' and E_0 are the dynamic stiffness of the SFF scaffolds and of the solid material respectively, P is the scaffold porosity, and α is a scaffold characteristic coefficient dependent on pore architecture. If the physicochemical properties of 3D scaffolds are also included in the mechanical characterization of the resulting structures, this model can be further expanded and dynamic stiffness E' predicted depending on the structural porosity P and the polymeric mesh size ξ as [103]:

$$E' = K \cdot e^{-0.5\left[\left(\frac{P + P_0}{C_1}\right)^2 + \left(\frac{\xi + \xi_0}{C_2}\right)^2\right]} \quad (2)$$

where the coefficients K, C_1, and C_2 are related to polymeric intrinsic parameters, such as the bulk dynamic stiffness E_0, the elastically effective network chain concentration ν_e, the number average molecular weight M_n and the cross-link molecular weight M_c. P_0 and ξ_0 are coefficients depending on the scaffold structural porosity P and on the polymer mesh size ξ.

Although scaffolds were characterized to mimic the elastic and plastic mechanical properties of cartilage (Fig. **2**), this model could be generalized to different tissues and biomaterials possessing different physicochemical properties

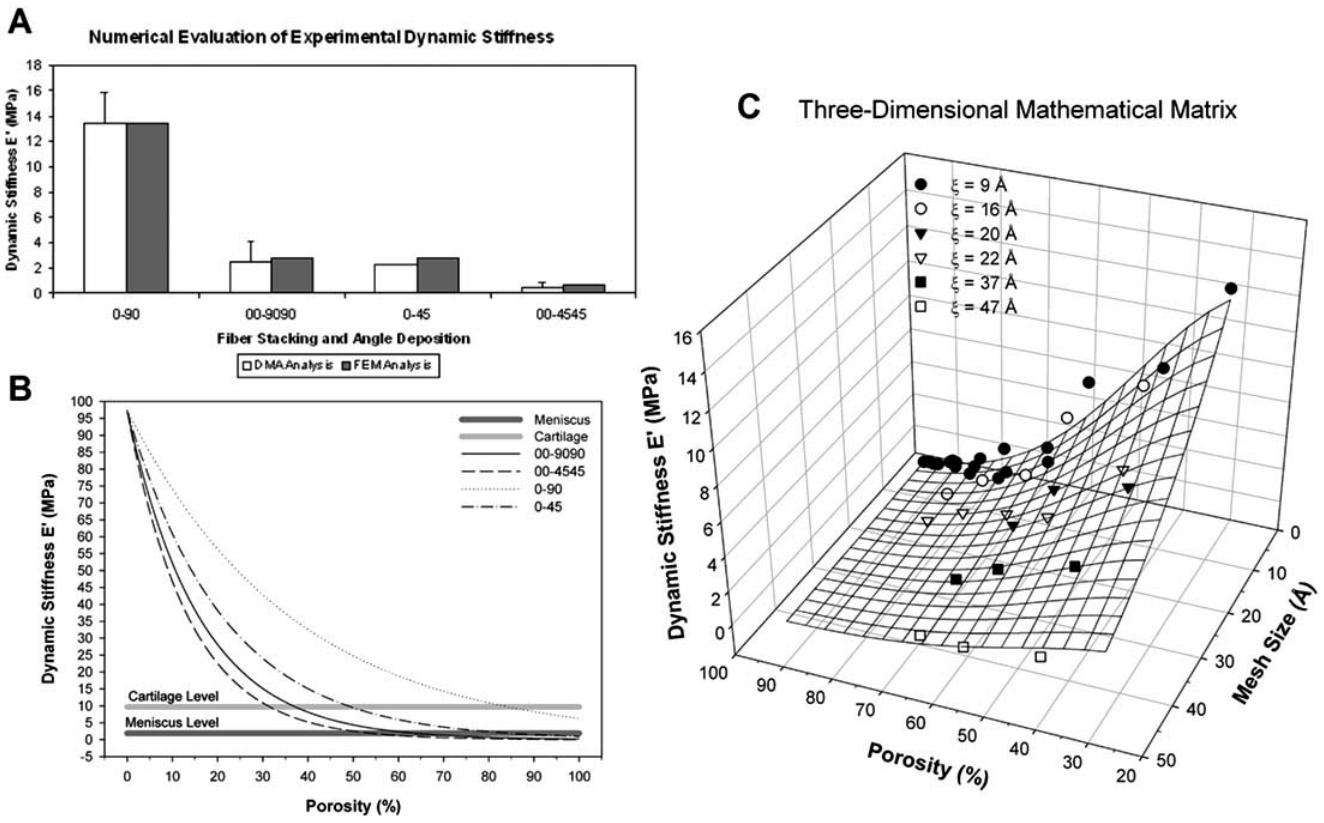

Fig. (2). Mathematical model to predict the dynamic stiffness of 3DF scaffolds. (**A**) Comparison between experimental (white) and computed (grey) bars. (**B**) Dynamic stiffness variation with porosity for different scaffold architectures. (**C**) Mathematical model predicting dynamic stiffness for given porosity and physicochemical biomaterials properties. (Adapted from Moroni *et al.* [103] with permission).

that could be used as scaffolds for a wider number of applications in regenerative medicine. Ultimately, this model could be used to predict the mechanical properties of a particular scaffold design, or conversely to decide which scaffold design could be used to match the mechanical, physicochemical, and the structural properties of a specific tissue to repair, restore, or regenerate. Yet, further light needs to be shed on the influence of different pore shape and scaffold architecture on tissue formation and guidance.

4. THE EFFECT OF SCAFFOLD COMPOSITION AND 3D PORE ARCHITECTURE ON CELL DIFFERENTIATION AND TISSUE FORMATION

In order to better understand the role of random versus designed pore architecture on tissue formation, two different scaffold architectures were fabricated *via* conventional compression moulding/salt leaching (CM) or 3DF technology from two different PEGT/PBT compositions (high PEG MW 1000/7030 and low PEG MW 300/55/45). This model system allowed us to investigate whether the re-differentiation and cartilage tissue formation capacity of adult human chondrocytes could be regulated by controlled modifications of scaffold composition and architecture.

With respect to understanding the role of composition on cell-biomaterial interactions and differentiation prior to moving to a 3D model, protein adsorption studies [108, 122] were performed on a range of 2D PEGT/PBT films, specifically related to the effects of composition on adsorption of the cell adhesion proteins fibronectin (FN) and vitronectin (VN). The premise surrounding these studies related to data suggesting that increased FN adsorption enhances cell spreading and de-differentiation [108, 122, 125]. PEGT/PBT films presenting a high PEG MW exhibited a low FN to VN adsorption ratio. In contrast, PEGT/PBT substrates with low PEG MW have shown preferential surface adsorption of FN compared to VN.

In a parallel study investigating the re-differentiation of expanded (passage 2) human nasal chondrocytes, we observed a direct relationship between cell adhesion, morphology and re-differentiation potential on 2D PEGT/PBT substrates *in vitro* [121]. There was a significant influence of PEGT/PBT composition on cell adhesion in the presence of both serum-containing (S+) or serum-free (SF) media (not shown). Low PEG MW 300/55/45 compositions supported cell adhesion and a spread cell morphology (Fig. **4C**, **D**) resulting in reduced cell re-differentiation capacity, as evidenced by low collagen II/I mRNA expression (Fig. **4**). Whereas, high PEG MW 1000/70/30 compositions promoted a more spherical cell morphology (Fig. **4A**, **B**), and increased collagen II/I mRNA expression (Fig. **4**) similar to mRNA levels in positive control samples for differentiated tissue obtained *via* pellet culture. Immunofluorescent staining for both $\alpha_5\beta_1$ fibronectin (FN) (Fig. **4B**, **D**) and $\alpha_V\beta_3$ vitronectin (VN) (Fig. **4A**, **C**) cell integrin receptors demonstrated clear differences with PEGT/PBT composition. There was a significantly greater number of FN integrin receptor expressing cells adhering to low PEG MW 300/55/45 films compared with VN [121], concomitant with the abovementioned re-

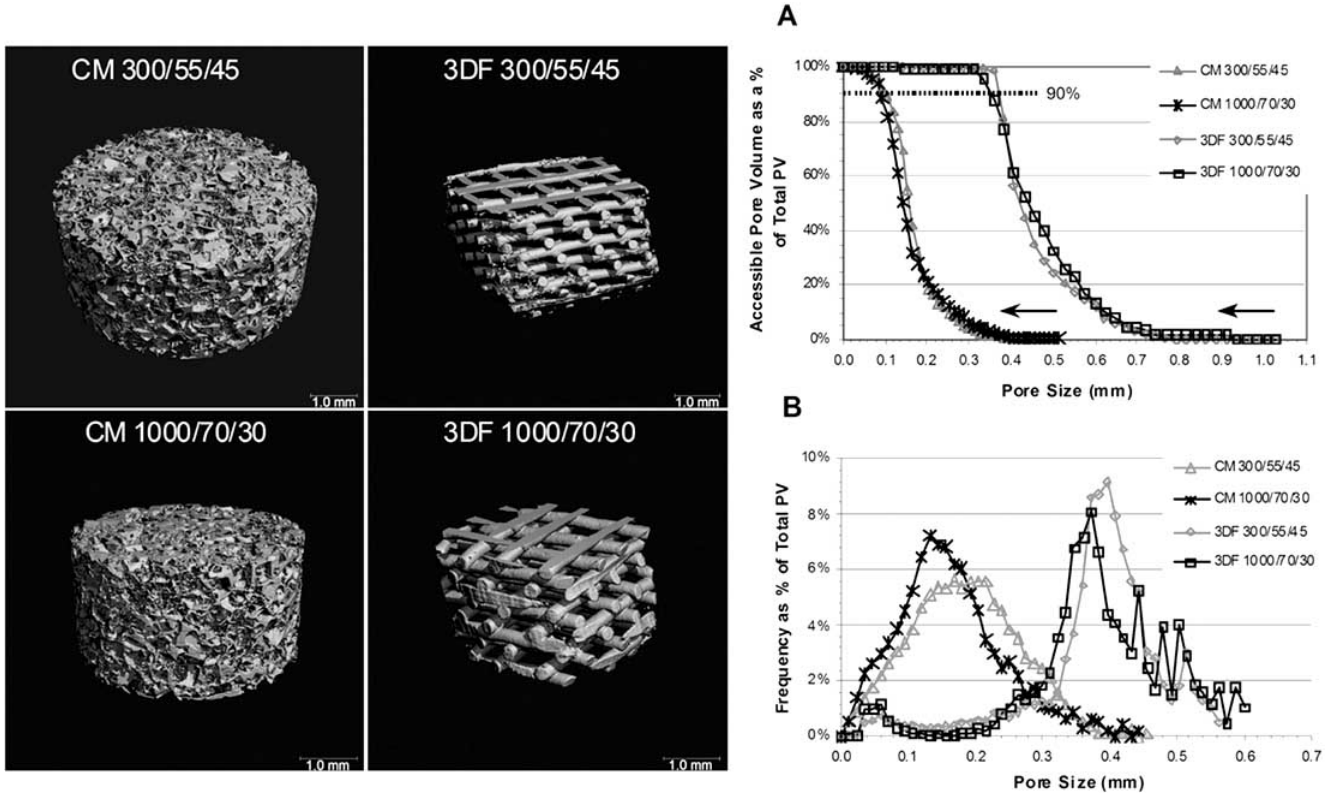

Fig. (3). 3D reconstruction of μCT scans of different PEGT/PBT compositions (300/55/45 and 1000/70/30) and scaffold architectures generated by compression moulding (CM) or 3D fibre deposition technique (3DF). (**A**) Accessible pore volume distribution, and (**B**) interconnecting pore size distribution data for both compositions of CM and 3DF scaffolds represented as a percentage of total pore volume (PV). The dotted line in (**A**) was used to determine the pore size at which 90% of the pore volume was accessible. With similar overall porosity, the average interconnecting pore size in 3DF scaffolds was double that of CM scaffolds. 3DF scaffolds also contain larger, more accessible pores. (Adapted from Miot, Woodfield *et al.* [37] with permission).

duced re-differentiation capacity. Whereas on high PEG MW 1000/70/30 films, cells formed spherical aggregates with similar numbers of cells expressing both FN and VN integrin receptor between cell-cell contacts.

The fact that lower PEG MW 300/55/45 compositions show preferential adsorption of FN compared to VN [108, 122] suggests that the surface of these PEGT/PBT substrates were FN-rich, thereby supporting cell adhesion and spread-

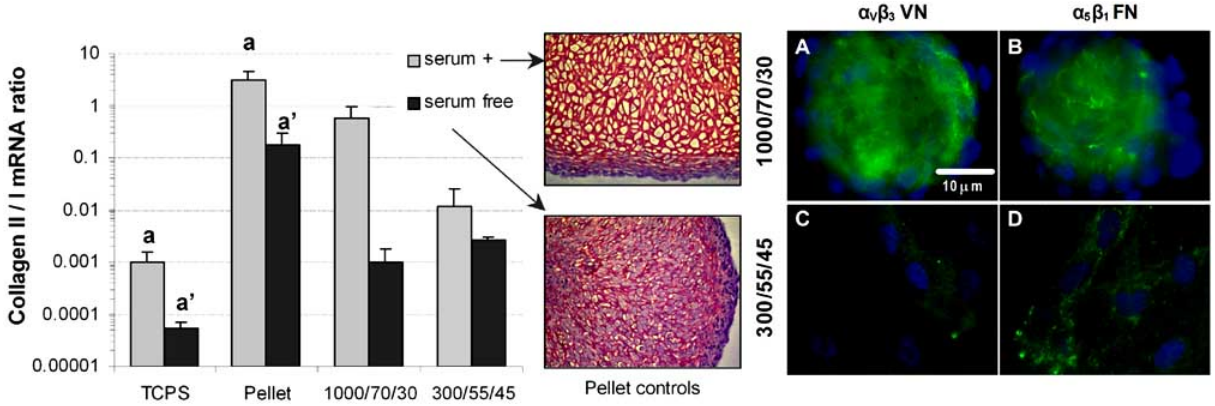

Fig. (4). Re-differentiation potential (collagen type II/I mRNA ratio) of expanded (P2) human nasal chondrocytes on 2D 1000/70/30 and 300/55/45 substrates after 10 days culture in serum containing (S+) or serum-free (SF) media. Negative control for re-differentiation = tissue culture polystyrene (TCPS); positive control for re-differentiation = pellet. Inset pictures show positive safranin-O staining in pellet cultures in both S+ and SF media (x100). Significant difference between substrates denoted by: S+ media = a ; SF media = a'. (**A**, **C**) Immunofluorescent staining for $\alpha_V\beta_3$ vitronectin and (**B**, **D**) $\alpha_5\beta_1$ fibronectin integrin receptors in expanded human nasal chondrocytes at day 10. Spherical cell aggregates formed on 1000/70/30 substrates (**A**, **B**) with high expression of both $\alpha_5\beta_1$ fibronectin (**A**) and $\alpha_V\beta_3$ vitronectin integrin receptors (**C**) from cell-cell contact, whereas spindle-shaped cells adhered to 300/55/45 substrates (**C**, **D**) expressing greater $\alpha_5\beta_1$ fibronectin integrin receptors (**D**) than $\alpha_V\beta_3$ vitronectin receptors (**C**). Cell nuclei counter stained with DAPI. (Adapted from Woodfield *et al.* [121] with permission).

ing, but detrimentally effecting the re-differentiation capacity of expanded human chondrocytes, whereas FN-deficient 1000/70/30 substrates enhanced re-differentiation capacity.

To further assess re-differentiation capacity in 3D, CM and 3DF scaffolds were produced for the two PEGT/PBT compositions with similar overall porosity but with inherently different interconnecting pore size. Micro-computed tomography (μCT) was adopted to accurately characterise scaffold porosity, volume fraction (i.e. surface area to volume ratio), interconnecting pore size and total accessible pore volume (Fig. **3**). The accessible pore volume distribution and pore size distribution for both 300/55/45 and 1000/70/30 compositions of CM and 3DF scaffolds are represented as a percentage of total pore volume (PV) in Fig. (**3**). The accessible pore volumes in both CM and 3DF scaffolds were approximately 100% interconnected. However, 3DF scaffolds had a considerably greater accessibility cut-off value of ~360 μm (taken as the pore size guaranteeing at least 90% of the pore volume was accessible) compared with ~100 μm in CM scaffolds (Fig. **3A**). Furthermore, as shown in Fig. (**3B**) and Table **1**, 300/55/45 and 1000/70/30 3DF scaffolds had considerably greater average pore sizes (388 μm and 380 μm respectively) than CM scaffolds (182 μm and 160 μm respectively). CM scaffolds also had 2-3 times greater volume fraction than 3DF scaffolds (Table **1**).

To give an indirect measure of scaffold tortuosity or complexity, 3D μCT analysis also allowed determination of a connectivity density (CD) index, which essentially counts the number of connections between pores for a given scaffold volume [126]. For CM scaffolds, the CD ranged between 246–408 (i.e. high tortuosity) as opposed to a range of approximately 5–7 (i.e. low tortuosity) in 3DF scaffolds. Given that 3DF scaffolds show a very low CD and a pore volume that is 90% accessible at pore sizes greater than 360μm demonstrates a simple, less tortuous pore architecture, whereas CM scaffolds exhibited a high CD and a pore volume that is 90% accessible at pore sizes greater than 100 μm, indicative of a more complex, tortuous pore architecture. This demonstrated that, with a similar overall porosity, designed 3DF scaffold architectures could be chosen with an average interconnecting pore size that was double that of the random CM scaffold architectures, whose interconnecting pore size was bound by salt granule size.

The effect of varying scaffold architecture and material composition (300/55/45 and 1000/70/30) on cell re-differentiation and cartilage formation are shown in Fig. (**5**). These results demonstrated that high MW PEGT/PBT compositions (e.g., 1000/70/30) supporting the maintenance of the chondrogenic phenotype on 2D films in previous studies [108, 121, 122] were also capable of promoting chondrocyte re-differentiation and cartilaginous matrix accumulation in porous CM and 3DF scaffolds *in vitro*. As illustrated in Fig. (**5**), 3DF scaffold architectures, with a more accessible pore volume and larger interconnecting pores, had greater amounts of positive safranin-O staining for GAG (Figs. **5B**, **4D**) and significantly increased GAG/DNA deposition (Fig. **5E**) compared to CM scaffolds (Figs. **5A**, **4C**), but only if a 1000/70/30 composition was used. Interestingly, enhanced collagen type II mRNA was observed in 3DF compared with CM scaffolds irrespective of composition (Fig. **5F**), suggesting that at the mRNA level, architecture alone is capable of instructing collagen type II synthesis pathways in human chondrocytes, and may operate independently to GAG synthesis pathways.

It is clear that biomaterial composition and scaffold architecture alone play a critical role in cell response and regulation of tissue formation. Our data suggests that, for tissue engineering approaches which expose 3D scaffolds to serum containing media, and thereby preferential protein adsorption, a FN-rich substrate-protein milieu promotes chondrocyte adhesion and a de-differentiated phenotype, whereas a FN-deficient substrate-protein milieu promotes a spherical morphology and maintenance of differentiated chondrocyte phenotype. When screened in combination, we observed synergistic effects of both composition and 3D scaffold architecture on the increased quality and quantity of cartilage tissue formation. In these specific studies, our data suggests that, comparatively, PEGT/PBT scaffold composition may have a more significant influence on cell differentiation and tissue formation than architecture alone. However, further combinatorial screening studies investigating a wider range of material compositions and architectures are necessary to further study cell response and ECM formation in a range of tissues.

5. THE EFFECT OF PORE SIZE GRADIENTS ON THE ZONAL COMPOSITION OF ENGINEERED TISSUES

Given the fact that controlled changes in scaffold architecture and composition can have a dramatic effect of the quantity and quality of tissue formation within different scaffolds, it is also interesting to study the effects of varying architecture (i.e. using a gradient in pore sizes) within a single scaffold. Not only would this provide a standardised and high throughput platform to screen cell-biomaterial interac-

Table 1. Structural Characterization of Scaffold Architecture Fabricated by Conventional Compression Moulding and Particulate Leaching (CM) or *via* 3D Fibre-Deposition (3DF)

Sample	Measured Vol% Porosity		Scaffold Vol. Fraction	Avg. Pore Size	Pore Size Range	Pore Size at ≥90% Accessible Pore Vol.
	m/V (%)	μCT (%)	μCT (mm^{-1})	μCT (μm)	μCT (μm)	μCT (μm)
CM 300/55/45	75.6 ± 1.9	81.8	10.0	182	6 – 450	98
CM 1000/70/30	76.0 ± 2.1	77.8	12.2	160	6 – 444	95
3DF 300/55/45	70.2 ± 1.2	74.4	3.8	380	132 – 450	380
3DF 1000/70/30	71.5 ± 1.8	71.2	4.0	388	156 – 600	360

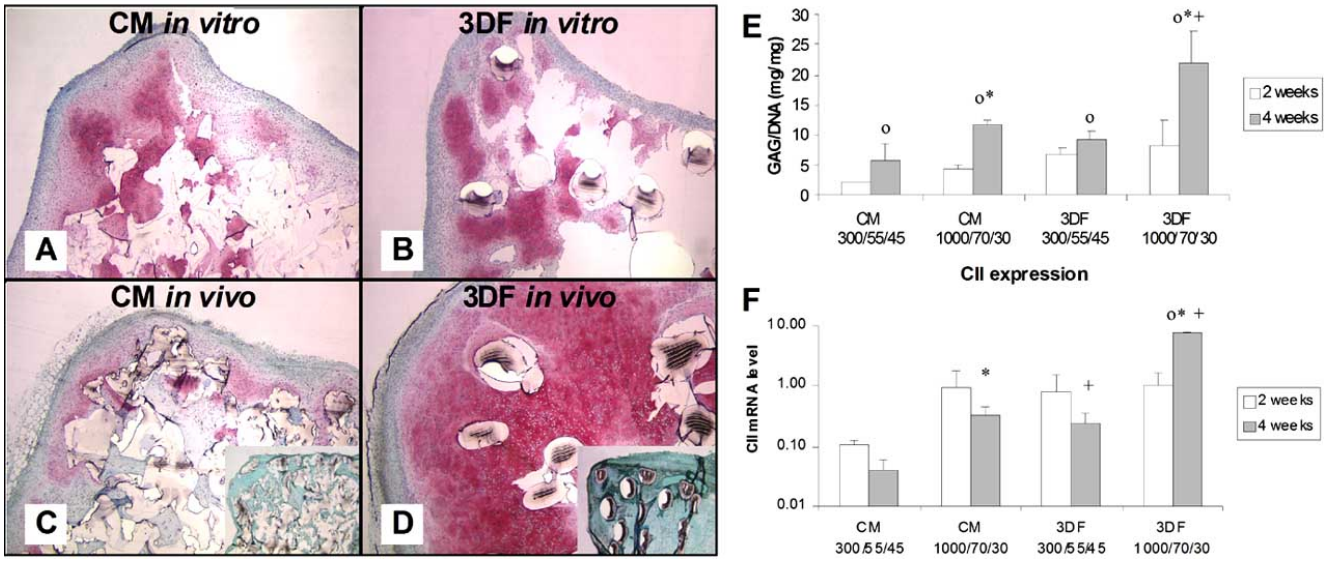

Fig. (5). Histological sections of tissue engineered constructs showing a significant increase in the amount and distribution of positive safranin-O staining for GAG between CM (**A**, **C**) and 3DF 300/55/45 scaffolds (**B**, **D**) following culture of bovine chondrocytes for 2 weeks *in vitro* (**A**, **B**) or 4 weeks subcutaneous implantation in nude mice *in vivo* (**C**, **D**). Inset in **C**, **D** show control scaffolds implanted without cells. (Adapted from Malda, Woodfield *et al.* [99] with permission). (**E**) GAG content normalized to the DNA amount of constructs generated by expanded human nasal chondrocytes cultured for 2 or 4 weeks in CM and 3DF scaffolds of both 300/55/45 and 1000/70/30 composition. (**F**) Collagen type II mRNA expression level in expanded human nasal chondrocytes cultured for 2 or 4 weeks in CM and 3DF scaffolds of both 300/55/45 and 1000/70/30 composition. Statistically significant differences ($p<0.05$) are indicated as follows: ***** = different from composition 300/55/45 for the same architecture; **+** = different from architecture CM for the same composition; **o** = different from 2 weeks of culture for the same architecture and composition. (Adapted from Miot, Woodfield *et al.* [37] with permission).

tions in 3D in the same population of cells in one scaffold, it also would allow the generation of tissue engineered constructs with zonal cell or ECM organisation more similar to native tissues, as well as gradients in composition and/or mechanical properties for example, compared to more traditional scaffolds with homogeneous characteristics.

By adapting the 3DF scaffold technology we designed and produced 100% interconnecting scaffolds containing either homogenously-spaced pores (1 mm fiber spacing, ≈Ø680 μm pore size) or pore-size gradients (0.5–2.0 mm fiber spacing, ≈Ø200–1650 μm range), but with similar overall porosity (≈80%) and volume fraction available for cell attachment and ECM formation (Fig. **6**). The rationale for the chosen zonal architecture was based on the characteristic superficial, middle and lower zones of native articular cartilage, each containing a variation in cell content, cell morphology and collagen orientation for example [16, 98].

In adopting this approach, it was possible to design model 3DF scaffolds containing: (a) homogenously-sized pores (1 mm spacing) or pore-size gradients (0.5-2.0 mm spacing), (b) similar scaffold volume fraction (i.e. surface to volume ratio) (1 mm: 3.25 mm^{-1}, Grad: 3.69 mm^{-1}), (c) similar overall porosity (1 mm: 80.1%, Grad: 78.0%) for cell attachment and ECM synthesis, and (d) a 100% interconnecting pore volume to promote cell infiltration and maximize nutrient/waste exchange throughout. As expected the *S* zone, with a 0.5 mm fibre spacing in *Grad* scaffolds, had the lowest porosity and highest volume fraction (59.2% and 6.67 mm^{-1} respectively), while the *L* zone, with a 2.0 mm fibre spacing, had the highest porosity and lowest volume fraction (87.4% and 2.05 mm^{-1} respectively). The middle *M* zone, with a 1.0 mm fibre spacing, had a porosity and volume fraction of 78.0% and 3.59 mm^{-1} respectively.

As a result, the ability of anisotropic pore architectures to influence the zonal organization of chondrocytes and ECM components could be investigated. This was achieved by quantitatively evaluating zonal chondrocyte distribution and organization of cartilage ECM components, as measured by DNA, GAG and collagen type II content, in response to these model scaffold geometries and seeding regimes following *in vitro* culture. Furthermore, zonal cell and ECM formation on scaffolds *in vitro* were compared with native bovine articular cartilage explants.

In vitro cell seeding showed that pore-size gradients promoted a similar anisotropic cell distribution as the superficial (S), middle (M) and lower (L) zones in immature bovine articular cartilage (Fig. **7A**, **B**). There was a direct correlation between zonal scaffold volume fraction with both DNA (Fig. **8A**) and GAG content (Fig. **8B**). Prolonged tissue culture in spinner flasks up to 21 days *in vitro* showed similar inhomogeneous distributions in zonal GAG (Figs. **7C**, **D**, **8E**, **F**) and collagen type II accumulation (Fig **7E**, **F**) but levels were an order of magnitude less than in native cartilage (Fig. **7D**, **F**). Gradients in cell-cell interactions based on controlled changes in pore size within *Grad* scaffolds did not influence the zonal distribution in the amount of GAG synthesised per cell (i.e. GAG/DNA – not shown).

The ability to control gradients in scaffold architecture such as interconnecting pore size, and volume fraction provided insight into ways in which instructive characteristics could be incorporated into 3D scaffold designs for tissue engineering articular cartilage which resembles the native

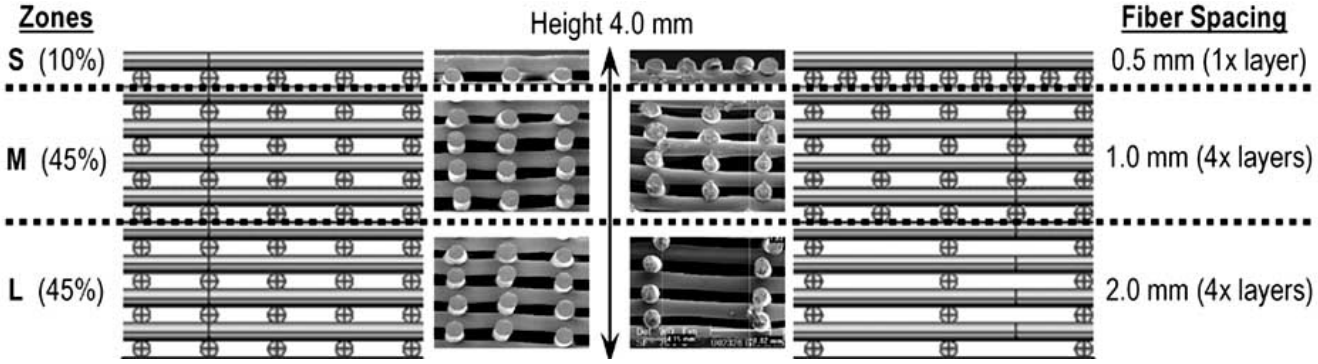

Fig. (6). Schematic and SEM cross-sections of model 3DF scaffolds containing either a homogeneous 1 mm fiber spacing (*1 mm*) or an anisotropic pore-size gradient (*Grad*). Regions corresponding to the upper (*S* – 10%), middle (*M* – 45%) and lower zones (*L* – 45%) are indicated on the left, while the associated fiber spacing used in *Grad* scaffolds (0.5, 1.0 and 2.0 mm) are indicated on the right. (Adapted from Woodfield *et al.* [98] with permission).

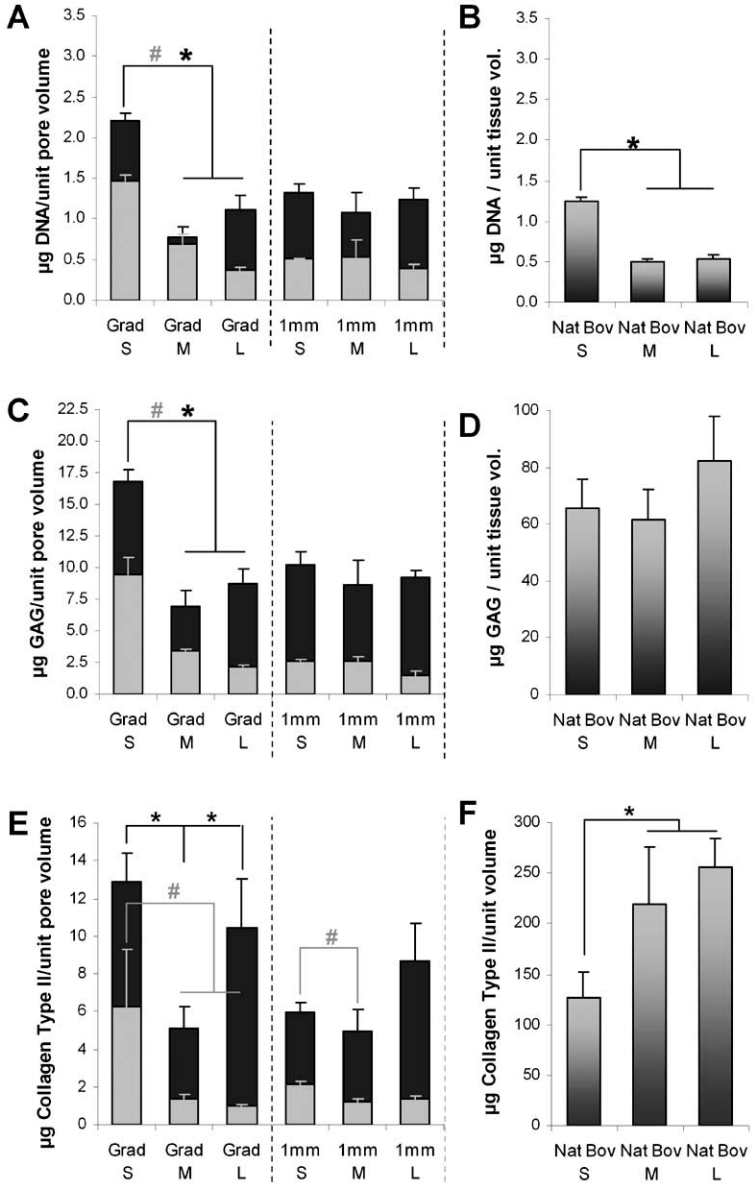

Fig. (7). Zonal distribution in cell number (**A**, **B**), GAG content (**C**, **D**), and collagen type II content (**E**, **F**) within *Grad* and *1 mm* constructs after seeding at day 3 (light grey bars ■) and 21 days tissue culture (dark grey bars ■) compared with native bovine articular cartilage explants (**B**, **D**, **F**). For each scaffold architecture, constructs were sectioned into their corresponding S (10%), M (45%) and L (45%) zones and analyzed separately. Significant difference between S, M and L zones denoted by: **#** = day 3, ***** = day 21. (Adapted from Woodfield *et al.* [98] with permission).

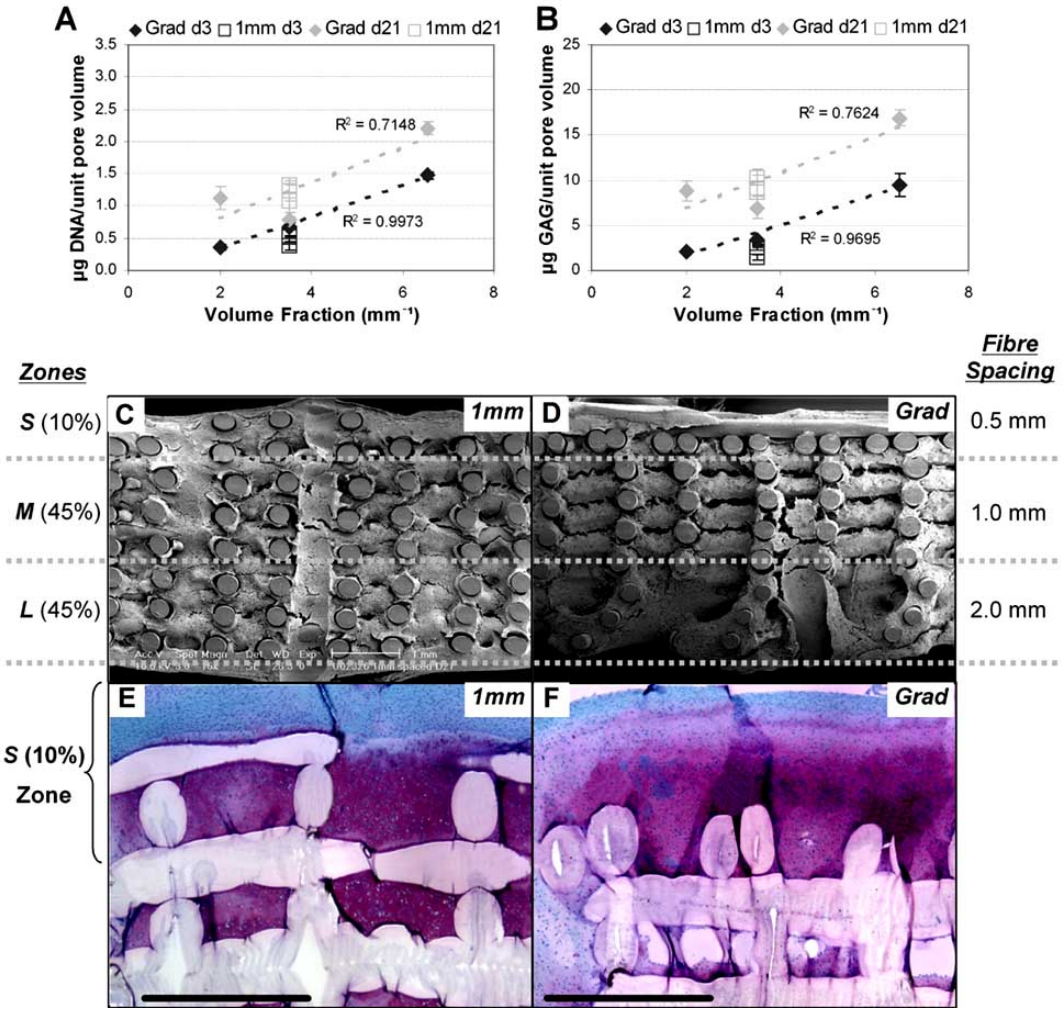

Fig. (8). (**A**) Correlation between cell number (DNA content), and (**B**) GAG content with scaffold volume fraction in *Grad* and *1 mm* scaffolds respectively after 3 days seeding and 21 days tissue culture. Representative SEM (**C**, **D**) and safranin-O sections (**E**, **F**) illustrate differences in extra cellular matrix (ECM) formation and distribution within *1 mm* (**C**, **E**) and *Grad* (**D**, **F**) scaffolds after 21 days culture. (Adapted from Woodfield *et al*. [98] with permission).

zonal cell, structural and mechanical organization. Using this experimental model, we illustrated how scaffold design and novel processing techniques can be used to develop anisotropic pore architectures for instructing zonal cell and tissue distribution in tissue engineered constructs.

6. THE EFFECT OF 3D PORE ARCHITECTURE ON NUTRIENT DIFFUSION IN ENGINEERED TISSUES

High-density cell cultures are often limited by inadequate supply of nutrients and limitation of nutrients is thus a major issue in the development of tissue-engineered implants of clinically relevant sizes. *In vitro* created constructs lack vascularity, often resulting in diffusion distances within these grafts in the order of multiple millimetres or even centimetres. In contrast, the *in vivo* diffusion distance between a capillary lumen and a cell membrane is rarely more than 20 to 200 µm [127]. Hence, pronounced nutrient gradients occur within tissue-engineered constructs [77, 128, 129], which limits the size of the formed tissue, since the cells within the graft all rely on the supply of nutrients and transport of waste products mainly by diffusion.

In tissue-engineered constructs, the limitation of oxygen has gained increasing attention [77, 128-133] in particular because (a) oxygen consumption by the cells is relatively high; (b) oxygen diffusion is relatively slow, and; (c) oxygen has a low solubility in the culture medium and needs to be constantly replenished. Thus, due to the relatively slow diffusion of oxygen through developing constructs and the consumption of nutrients by the cells inside the constructs, nutrient gradients will still occur, even in situations where sufficient oxygen for the cells could be delivered to the surface of the construct.

Cartilaginous constructs based on CM and 3DF scaffolds were used to illustrate that oxygen concentrations within tissue-engineered grafts rapidly decrease going from the exterior to the interior and intensify during the early stages of tissue development [77, 128, 131]. By means of oxygen microelectrode measurements, we confirmed that oxygen gradients were present within both polymer-cartilage constructs, *in vitro* as well as *in vivo* and these gradients intensify during the first 14 days of culture (Fig. **9**).This was associated with an increased cell density, resulting in a higher overall consumption in combination with matrix formation within the

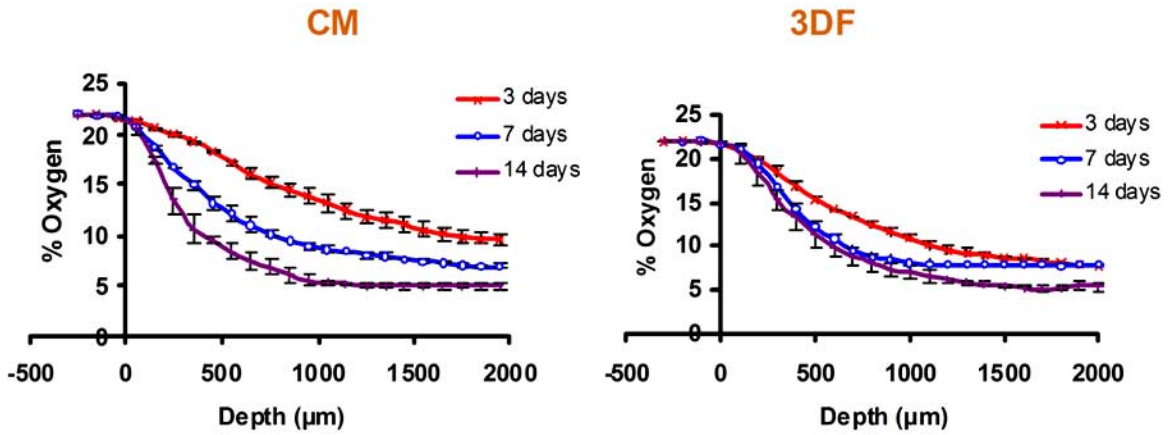

Fig. (9). Oxygen concentrations rapidly decrease from the exterior to the interior of both CM and 3DF cartilage constructs and intensify during the first 14 days of culture as was measured with an oxygen microelectrode. (Adapted from Malda *et al.* [77] with permission).

pores, blocking any potential convection through the scaffold and, thus, potentially decreasing the permeability of nutrients within the construct [130, 134]. Despite the organized pores of the 3DF scaffolds with its less tortuous and more open structure, this did not result in a less pronounced oxygen gradient compared to those in the CM counterparts. However, significantly more cells were present within the inner regions of the 3DF scaffolds and cartilage-like tissue deposition with a more homogeneous cell distribution *in vivo* was observed.

This observed higher cartilage matrix production within 3DF scaffolds after bioreactor culture and subsequent subcutaneous implantation in nude mice could be attributed to a number of factors, including the improved cell aggregation due to the smaller surface-to-volume ratio. However, in view of the similar oxygen profile and the additional higher cell content in the inner regions, this also indicates the improved accessibility for nutrients.

To further reveal the relation between the oxygen gradient and the spatial cell distribution, a mathematical model was developed that describes the interaction between the spatially and temporally evolving oxygen profiles and cell distributions within these constructs [130]. Mathematical analysis of the outcomes of several studies using 3-dimensional (3D) tissue constructs, such as tumour spheroids [135] or engineered cardiac tissue [128], have revealed that the supply of nutrients to the cells in the construct can play a dominant role in the regulation and distribution of proliferation and differentiation in the context of *in vitro* cultures. Lewis *et al.* [130] evaluated specifically the heterogeneous proliferation of chondrocytes within a 3D scaffold structure with the purpose of improving protocols for engineered tissue growth. A simple mathematical model was developed to examine the very strong interaction between evolving oxygen profiles and cell distributions within cartilaginous constructs. A comparison between predictions of both spatial and temporal evolution of the oxygen tension and cell number density based on the model and experimental evidence showed that behaviour for the first 14 days can be explained well by the simple mathematical model (Fig. **10**). Interestingly, the results demonstrated that clinically relevant cell-scaffold constructs that rely solely on diffusion for their supply of nutrients will inevitably produce proliferation-dominated regions near the outer edge of the scaffold. Further this work has indicated that there is a direct relation between pore architecture, particularly the interconnections, and the governing oxygen gradients.

This study has provided further understanding of role of nutrient gradients and its relation to scaffold architecture. Additional modelling and experimental studies of the supply of other nutrients (e.g., glucose) and the removal of waste products (e.g., lactate) will yield further critical information on the role of inadequate mass transfer during the development of tissue engineered constructs. Critically, cell distribution and matrix deposition could be enhanced in 3DF scaffolds, stressing the importance of a rationally designed scaffold for cartilage tissue-engineering applications that offers possibilities for regulation of nutrient supply.

7. THE EFFECT OF BI-PHASIC COMPOSITION AND 3D PORE ARCHITECTURE ON TISSUE FORMATION AND GROWTH FACTOR RELEASE

As previously discussed in this paper, a number of requirements have to be generally satisfied when designing scaffolds for tissue engineering and regenerative medicine applications. Within these prerequisites, constructs must be biocompatible, possibly biodegradable and/or bioresorbable to minimize a foreign body reaction and to gradually disappear while the natural tissue is regenerating. They also have to offer an initial and adequate mechanical support for the seeded cells to integrate with the surrounding tissue and they have to provide the appropriate chemistry to direct cells and the ECM produced by them into the proper original tissue structure and architecture. Last, it would be favourable if they could facilitate regaining the original shape of the treated defect. Among the scaffold fabrication techniques nowadays accessible, RP systems have shown to be the most promising to satisfy all of these requirements, as they can process a large number of biomaterials [74, 93, 106, 136, 137] in a custom-made shape and with matching mechanical properties in comparison with the specific application considered [94, 103, 138], as also earlier treated. RP scaffolds normally possess fine tunable porosity, pore size and shape, and have a completely interconnected pore network, which allows a more efficient cell migration and nutrient perfusion than scaffolds fabricated with conventional textile or porogen techniques.

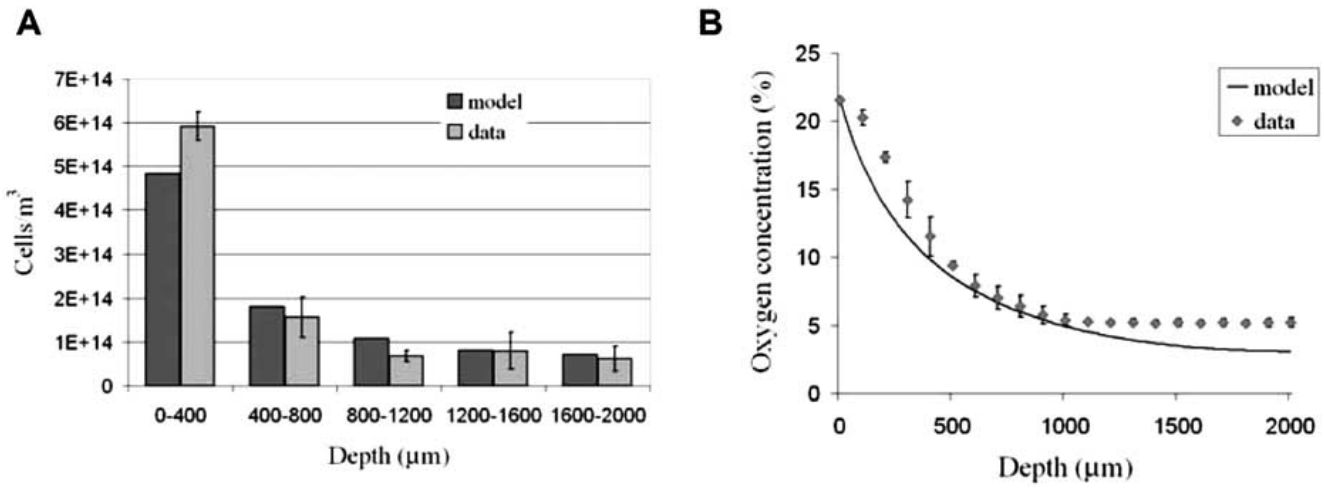

Fig. (10). Cell number densities (**A**) and oxygen concentrations (**B**) within cartilaginous constructs: comparison between the experimental data and model predictions on day 14. (Reproduced from Lewis *et al.* [130] with permission).

However, combining scaffolds with adequate mechanical and physicochemical properties is often critical. It is frequently the case that when the mechanical properties are appropriate, the physico-chemical characteristics of the scaffolds are insufficient due to either biomaterial processing or to the intrinsic chemistry of the material itself. Equally, when physicochemical properties are suitable, the scaffolds may not display an adequate mechanical behavior. From recent studies, it seems that the most optimal strategy in designing scaffolds for tissue engineering could pass through the integration of different biomaterials and of different fabrication technologies to combine mechanical, physicochemical, and biological cues at the macro, micro, and nano scale. From this perspective, 3DF and RP platforms could be ideal to preventively screen the best performing combination of biomaterials and RP technologies that enables satisfying all the tenets required for instructive and bioactive scaffolds. An example of different biomaterial integration to generate smart 3D scaffolds consisted in rapid prototyping polymeric blends with specific melt viscosities to create shell-core fibrous 3D scaffolds with favourable mechanical and physcicochemical properties to regenerate cartilage [104]. These shell-core scaffolds are comprised of a core-polymer that offers optimal mechanical properties to sustain articular cartilage loads and of a shell-polymer that was shown to maintain the appropriate interactions with chondrocytes preserving their native morphology [32, 108, 121, 122]. By varying the shell-core polymer compositions the controlled release of drugs, growth factors, or generally biofactors could be envisioned through diffusion or degradation of the shell and the of the core layers. Alternatively, a 3D system of drug reservoirs could be generated by selectively leaching the core-polymer and by capping the resulting hollow fibers. This approach has shown to modulate the release of a model protein as lyzozyme over a month period [102]. Similarly, exploiting the same process known as viscous encapsulation, 3D scaffolds with a ceramic coating of biphasic calcium phosphate (BCP) could be fabricated and may find similar instructive applications for bone tissue engineering (Fig. **11**). Integrating different physicochemical properties of polymers into shell-core RP scaffold architecture would result in regional release of biomolecules that are typically administered to enhance tissue formation and development. From this perspective, the combination of CAD/CAM designed matrices with biomaterials having different drug releasing capacities will allow controlling the presence in time and in space of these signals in a 3D tissue construct and might be appealing in the further regeneration and organization of more complex or hierarchical tissues.

A different solution to combine satisfactory mechanical and physicochemical properties could be offered by integrat-

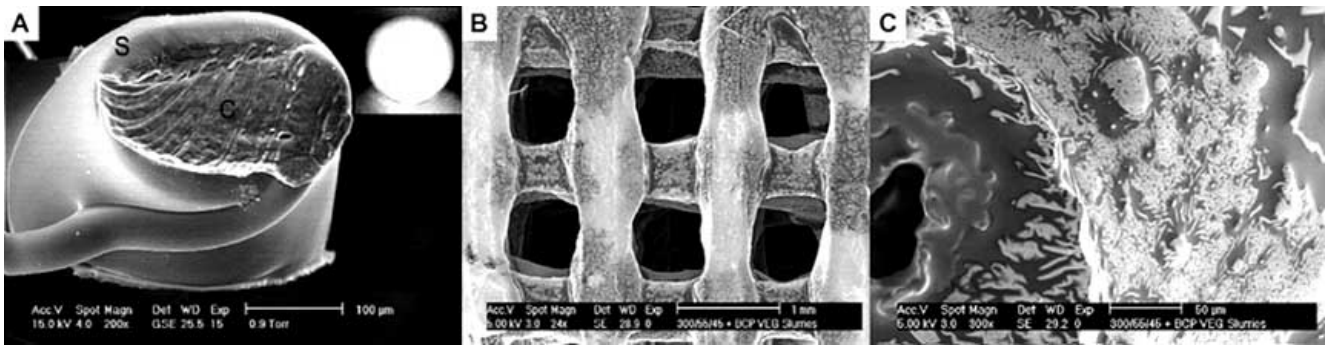

Fig. (11). ESEM micrographs of shell-core 3DF scaffolds with a 1000/70/30 (**A**) or a BCP ceramic (**B**) coating shell-layer over a polymeric 300/55/45 core fiber. Insert in (**A**) shows an incident microscopy image of a shell-core fiber where the more amorphous polymer used as a shell (s) layer is less birefringent and darker compared to the more crystalline core (c) polymer. (B) BCP-300/5545 top surface and (**C**) close-up on a fiber edge along the structure cross-section showing the ceramic phase at the surface. Scale bars: (**A**) 100 μm; (**B**) 1 mm; (**C**) 50 μm.

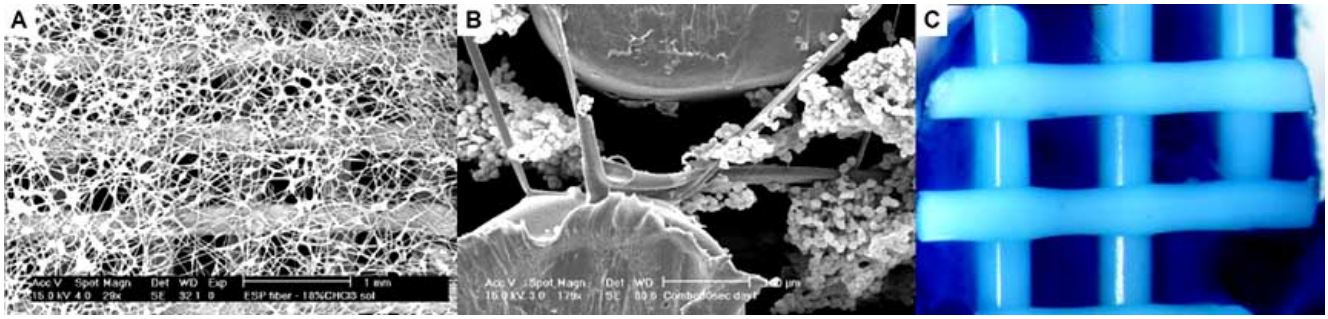

Fig. (12). 3DF and electrospun (ESP) integrated scaffolds. (**A**) SEM of the integrated fibrillar network along the X-Y scaffold plane; scale bar: 1 mm. (**B**) cross-section view of chondrocytes entrapped in the microfibrillar ESP network within the 3DF macrostructure; scale bar: 100 μm. (**C**) optical image of stem cells stained by methylene blue adhering on the ESP network integrated in the 3DF scaffold.

ing physical cues at different scales [139]. In this respect, electrospun fibers display features at the micro and nano scale, which are similar to the extra cellular matrix (ECM) dimensions. These scaffolds have shown to enhance cell proliferation and direct cell morphology depending on their surface topology [123, 140, 141]. Although they are highly performing in tension, their mechanical properties in compression are poor. Therefore, the integration of these fibrous porous networks in RP scaffolds would result in the fabrication of smart 3D constructs with adequate mechanical (RP macrostructure in compression; electrospun microstructure in tension) and physicochemical (electrospun fibrous topology) properties. These integrated scaffolds have been studied for cartilage regeneration and showed enhanced tissue formation, characteristic cell phenotype and morphology, and favourable mechanical properties.

Furthermore, the integration of the electrospun network sensibly improved cell attachment when stem cells were considered and seeded on the combined scaffolds (Fig. **12**). Although these are preliminary studies and further insights on hierarchical structures and their beneficial use in tissue engineering should be obtained, it appears that a combinatorial approach in scaffold design could generate better instructive templates for tissue regeneration and might also help to enlarge our understanding of fundamental biological phenomena.

8. DISCUSSION

One challenge in the design of biomaterials and scaffolds for tissue engineering and regenerative medicine is to understand the fundamental cell and tissue processes involved in forming functional 3D tissues. In this article, we illustrated that there are many factors involved in developing porous biomaterial scaffolds, and many of them are interdependent in some shape or form.

Based on the increasing evidence emerging in literature, it is becoming less clear what definitive conclusions can be drawn from studies comparing tissue formation on various scaffolds or biomaterials with 3D architectures produced using typical random processing methods such as foaming, particulate leaching and non-woven fibre meshes [101]. As we have demonstrated, some examples of interdependent factors controlling 3D tissue formation include: porosity, interconnecting pore size, permeability, volume fraction, nutrient and growth factor diffusion, waste exchange, nutrient consumption rate, cell density and distribution, cell-cell and cell-biomaterial interaction, biomaterial composition and degradation rate, protein adsorption and mechanical properties. Minor variations or random distributions of interconnecting pore size influence cell seeding capacity and results in less homogeneous cell distribution and fewer cell-cell interactions. This in turn biases nutrient gradients thereby critically affecting cell viability as well as the quality and quantity of tissue formed. Variable tissue formation ultimately influences construct mechanical properties as will variable scaffold degradation rate without accurate control over designed scaffold architecture and composition. One further consideration when screening biomaterials and scaffold architectures is the clinically relevant size and shape of the desired construct, which is often an order of magnitude (or more) greater in scale to those assessed experimentally. Again, scale limitations influence many of the interdependent factors described above (e.g., cell numbers and distances for nutrient diffusion).

One limitation of the 3DF process described herein is that of fibre size (typically Ø150 - 250μm) – a scale at which a single cell would likely "see" as a 2D surface. One solution to these issues of scale was to produce bi-phasic scaffolds containing 3DF macro-fibres and ESP nano-fibres. Furthermore, chondrocytes behave differently in 2D (cell-biomaterial interaction) versus in an 3D aggregate ("community effect" *via* cell-cell interaction). Apart from the physical structure of the scaffold and the typical 2D surface interactions between adsorbed proteins, peptides and cells for example, cells also "see" and respond to the 3D porous space, as well as other cells and varying nutrient gradients. Our studies suggest that it is the "smart design" of that 3D pore architecture, not just the physical scaffold itself, that plays a critical role in directing cell behaviour (as demonstrated earlier in Sections 4-7).

We have described a number of model systems adopting smart scaffold design and RP/SFF processing technology to asses the effect of cell-biomaterial interactions and tissue formation in 3D in a controlled manner. While techniques adopted in these studies may not be defined as high-throughput *per se*, there are a number of advantages to the model systems described herein that are relevant or could be simply modified in order to expand screening capabilities, and are discussed in more detail below.

RP/SFF techniques allow simple homogeneous structures to be developed as well as complex anisotropic structures into a single scaffold with controlled pore size, shape and interconnectivity. Furthermore, the layer-by-layer process allows freedom to alter one or many of these parameters in 3D in a range of biomaterials. With respect to 3DF techniques described in this review, in addition to varying scaffold fibre spacing, multiple nozzles and/or syringes could be added and interchanged during processing in the future in order to deposit fibres with different diameter and PEGT/PBT composition. As a result, interconnecting pore size, volume fraction, fibre orientation, surface chemistry, degradation behaviour and mechanical properties could be controlled from one layer to another. In all these cases, the ability to produce anatomically-shaped or customized implants may provide a significant clinical impact [142, 143]. It has been recognised that to date, most work on high-throughput screening based on cellular function has largely ignored the biological context in which the cells are screened and in which bioactive molecules are displayed [6]. In this regard, arrays of multi-phasic or multi-zonal scaffolds could be manufactured in order to screen a range of cell-biomaterial interactions or biomaterial-protein milieu profiles using homogeneous or heterogeneous cell populations in 3D. Controlled variations or gradients in zonal architecture, volume fraction or biomaterial composition, for example, could be implemented in a single 3D scaffold and exposed to a single cell type or screened for preferential adsorption of protein(s). Similarly, combinatorial arrays or libraries of designed 3D scaffolds individually expressing controlled variations in architecture or biomaterial composition could be exposed to single or multiple cell types or screen various adsorbed proteins similar to 2D high-throughput models described recently [8, 27]. For example, specific biomaterial compositions or 3D architectures (or combinations thereof) that are able to induce adult or embryonic stem cell differentiation towards a specific desired phenotype could be identified using these approaches.

RP/SFF techniques allow simple structures with homogeneous composition to be developed as well as complex multi-phasic structures including incorporation of single or multiple growth factors with single or multiple release profiles. Again, as described they consent freedom to alter one or many parameters within layers or between layers of the 3D scaffold architecture. This may be important in the development of biomaterials for drug delivery, particularly in complex 3D structures where multiple growth factors or certain regions within the scaffold require incorporation of bioactive signals (either matrix bound or incorporated *via* viscous encapsulation/hollow fibre techniques). Yet further, known release profiles or biomaterial degradation rate across gradient structures or compositions could be determined experimentally *in vitro* and then incorporated into computational models to better predict or optimise scaffold function *in vivo* [144].

RP/SFF techniques allow simple homogeneous architectures to be developed offering isotropic mechanical properties as well as complex anisotropic architectures with varying mechanical properties throughout the scaffold to complement the anisotropic mechanical properties of human tissues [136, 145]. As demonstrated in this review, a library of static and dynamic mechanical characteristics for 3DF PEGT/PBT architectures were obtained which can be incorporated into calculations predicting the response of new scaffold designs.

In this light, computational studies based on topology optimisation of scaffold architecture for tissue engineering applications have emerged. Given that RP/SFF techniques allow almost any micro architecture to be manufactured with high accuracy, it begs the question then as to what is the most optimal architecture for a given biomaterial to promote formation of a desired tissue for its desired application *in vivo*? Studies by Hollister and co-workers have developed algorithms based on optimising porous architectures balancing mechanical properties with porosity or permeability [93, 94, 136, 144-148], and more recently with predicted biomaterial degradation rate [144]. Furthermore, the incorporation of models to predict the diffusion and consumption of nutrients (such as glucose and oxygen, as described earlier), as well as how nutrient gradients effect cellular function and viability for a given scaffold architecture of clinically relevant size is critically important. High-throughput screening to develop a library of nutrient diffusion profiles would be an extremely powerful tool in developing models predicting tissue formation in designed scaffold architectures.

Additional advantages of being able to accurately produce porous 3D architectures from computer (CAD) models, or models directly from computed tomography (CT) scans of scaffolds, is that many physical properties such as porosity, volume fraction, mechanical properties, oxygen diffusion, degradation rate can all be modelled computationally. This is also the case for determining scaffold tortuosity [149] and permeability [150] providing further evidence of how high-throughput (or libraries) of physical scaffold properties and complex architecture can be achieved *via* computer modelling, which in turn can be directly married to high-throughput cell studies.

All of these abovementioned options allow more detailed and systematic *in vitro* and *in vivo* model systems to be developed and modelled, which will subsequently reduce the time and cost involved in performing large numbers of experiments to screen subtle changes in cell-biomaterial and cell-protein interactions, as well as biological response to scaffold parameters in 3D. With the increasing adoption of computational topology optimisation and models to describe scaffold properties, we still suggest that quickly and accurately measuring cell response in a high-throughput manner in 3D will continue to provide the greatest challenge. Given the current interest however, the continued development of combinatorial and high-throughput methods will have a large impact on the screening of biomaterials and 3D scaffolds for use in tissue engineering and regenerative medicine.

ACKNOWLEDGEMENTS

The authors would like to acknowledge the European Commission (FP5 project "SCAFCART" G5RD-CT-1999-00050 and FP6 project "INTELLISCAF" GSRD-2002-00697) for financially supporting aspects of this research (TW, LM). Dr. Malda is supported by a VENI fellowship from the Dutch Technology Foundation STW, Applied Science Division of NWO and the Technology Program of the Ministry of Economic Affairs.

REFERENCES

[1] Simon, C. G., Jr.; Stephens, J. S.; Dorsey, S. M.; Becker, M. L. Fabrication of combinatorial polymer scaffold libraries. *Rev. Sci. Instrum.*, **2007**, *78*(7), 072207.

[2] Zapata, P.; Su, J.; Garcia, A. J.; Meredith, J. C. Quantitative high-throughput screening of osteoblast attachment, spreading, and proliferation on demixed polymer blend micropatterns. *Biomacromolecules*, **2007**, *8*(6), 1907-17.

[3] Nakajima, M.; Ishimuro, T.; Kato, K.; Ko, I. K.; Hirata, I.; Arima, Y.; Iwata, H. Combinatorial protein display for the cell-based screening of biomaterials that direct neural stem cell differentiation. *Biomaterials*, **2007**, *28*(6), 1048-60.

[4] Albrecht, D. R.; Tsang, V. L.; Sah, R. L.; Bhatia, S. N. Photo- and electropatterning of hydrogel-encapsulated living cell arrays. *Lab Chip*, **2005**, *5*(1), 111-8.

[5] Simon, C. G., Jr.; Eidelman, N.; Kennedy, S. B.; Sehgal, A.; Khatri, C. A.; Washburn, N. R. Combinatorial screening of cell proliferation on poly(L-lactic acid)/poly(D,L-lactic acid) blends. *Biomaterials*, **2005**, *26*(34), 6906-15.

[6] Hubbell, J. A. Biomaterials science and high-throughput screening. *Nat. Biotechnol.*, **2004**, *22*(7), 828-9.

[7] Kohn, J. New approaches to biomaterials design. *Nat. Mater.*, **2004**, *3*(11), 745-7.

[8] Anderson, D. G.; Levenberg, S.; Langer, R. Nanoliter-scale synthesis of arrayed biomaterials and application to human embryonic stem cells. *Nat. Biotechnol.*, **2004**, *22*(7), 863-6.

[9] Weber, N.; Bolikal, D.; Bourke, S. L.; Kohn, J. Small changes in the polymer structure influence the adsorption behavior of fibrinogen on polymer surfaces: validation of a new rapid screening technique. *J. Biomed. Mater. Res. A*, **2004**, *68*(3), 496-503.

[10] Sarikaya, M.; Tamerler, C.; Jen, A. K.; Schulten, K.; Baneyx, F. Molecular biomimetics: nanotechnology through biology. *Nat. Mater.*, **2003**, *2*(9), 577-85.

[11] Meredith, J. C.; Sormana, J. L.; Keselowsky, B. G.; Garcia, A. J.; Tona, A.; Karim, A.; Amis, E. J. Combinatorial characterization of cell interactions with polymer surfaces. *J. Biomed. Mater. Res A*, **2003**, *66*(3), 483-90.

[12] Chen, T.; Vazquez-Duhalt, R.; Wu, C. F.; Bentley, W. E.; Payne, G. F. Combinatorial screening for enzyme-mediated coupling. Tyrosinase-catalyzed coupling to create protein--chitosan conjugates. *Biomacromolecules*, **2001**, *2*(2), 456-62.

[13] Santini, J.; Richards, A.; Scheidt, R.; Cima, M.; Langer, R. Microchips as Controlled Drug-Delivery Devices. *Angew. Chem. Int. Ed. Engl.*, **2000**, *39*(14), 2396-2407.

[14] Brocchini, S.; James, K.; Tangpasuthadol, V.; Kohn, J. Structure-property correlations in a combinatorial library of degradable biomaterials. *J. Biomed. Mater. Res.*, **1998**, *42*(1), 66-75.

[15] Lysaght, M. J.; Reyes, J. The growth of tissue engineering. *Tissue Eng.*, **2001**, *7*(5), 485-93.

[16] Woodfield, T. B. F.; Bezemer, J. M.; Pieper, J. S.; van Blitterswijk, C. A.; Riesle, J. Scaffolds for tissue engineering of cartilage. *Crit. Rev. Eukaryot. Gene. Expr.*, **2002**, *12*(3), 209-36.

[17] Hunziker, E. B. Tissue engineering of bone and cartilage. From the preclinical model to the patient. *Novartis. Found. Symp.*, **2003**, *249*, 70-8; discussion 78-85, 170-4, 239-41.

[18] Hunziker, E. B. Articular cartilage repair: basic science and clinical progress. A review of the current status and prospects. *Osteoarthritis Cartilage*, **2002**, *10*(6), 432-63.

[19] Langer, R.; Vacanti, J. P. Tissue engineering. *Science*, **1993**, *260*(5110), 920-6.

[20] Langer, R.; Tirrell, D. A. Designing materials for biology and medicine. *Nature*, **2004**, *428*(6982), 487-492.

[21] Niklason, L.; Langer, R. Prospects for organ and tissue replacement. *JAMA*, **2001**, *285*(5), 573-6.

[22] Kuo, C. K.; Li, W. J.; Mauck, R. L.; Tuan, R. S. Cartilage tissue engineering: its potential and uses. *Curr. Opin. Rheumatol.*, **2006**, *18*(1), 64-73.

[23] Hunziker, E. B. Articular cartilage repair: are the intrinsic biological constraints undermining this process insuperable? *Osteoarthritis Cartilage*, **1999**, *7*(1), 15-28.

[24] Hunziker, E. B. Biologic repair of articular cartilage. Defect models in experimental animals and matrix requirements. *Clin. Orthop.*, **1999**, *367*(Suppl), S135-46.

[25] Hung, C. T.; Mauck, R. L.; Wang, C. C.; Lima, E. G.; Ateshian, G. A. A paradigm for functional tissue engineering of articular cartilage *via* applied physiologic deformational loading. *Ann. Biomed. Eng.*, **2004**, *32*(1), 35-49.

[26] Butler, D.; Goldstein, S.; Guilak, F. Functional tissue engineering: the role of biomechanics. *J. Biomech. Eng.*, **2000**, *122*(6), 570-5.

[27] Anderson, D. G.; Putnam, D.; Lavik, E. B.; Mahmood, T. A.; Langer, R. Biomaterial microarrays: rapid, microscale screening of polymer-cell interaction. *Biomaterials*, **2005**, *26*(23), 4892-7.

[28] Hambleton, J.; Schwartz, Z.; Khare, A.; Windeler, S. W.; Luna, M.; Brooks, B. P.; Dean, D. D.; Boyan, B. D. Culture surfaces coated with various implant materials affect chondrocyte growth and metabolism. *J. Orthop. Res.*, **1994**, *12*(4), 542-52.

[29] Ishaug-Riley, S. L.; Okun, L. E.; Prado, G.; Applegate, M. A.; Ratcliffe, A. Human articular chondrocyte adhesion and proliferation on synthetic biodegradable polymer films. *Biomaterials*, **1999**, *20*(23-24), 2245-56.

[30] Lahiji, A.; Sohrabi, A.; Hungerford, D.; Frondoza, C. Chitosan supports the expression of extracellular matrix proteins in human osteoblasts and chondrocytes. *J. Biomed. Mater. Res.*, **2000**, *51*(4), 586-95.

[31] Lee, S.; Khang, G.; Lee, Y.; Lee, H. Interaction of human chondrocytes and NIH/3T3 fibroblasts on chloric acid-treated biodegradable polymer surfaces. *J. Biomater. Sci. Polym. Ed.*, **2002**, *13*(2), 197-212.

[32] Papadaki, M.; Mahmood, T.; Gupta, P.; Claase, M. B.; Grijpma, D. W.; Riesle, J.; van Blitterswijk, C. A.; Langer, R. The different behaviors of skeletal muscle cells and chondrocytes on PEGT/PBT block copolymers are related to the surface properties of the substrate. *J. Biomed. Mater. Res.*, **2001**, *54*(1), 47-58.

[33] Cukierman, E.; Pankov, R.; Stevens, D. R.; Yamada, K. M. Taking cell-matrix adhesions to the third dimension. *Science*, **2001**, *294*(5547), 1708-12.

[34] Sun, T.; Jackson, S.; Haycock, J. W.; MacNeil, S. Culture of skin cells in 3D rather than 2D improves their ability to survive exposure to cytotoxic agents. *J. Biotechnol.*, **2006**, *122*(3), 372-81.

[35] Birgersdotter, A.; Sandberg, R.; Ernberg, I. Gene expression perturbation *in vitro*--a growing case for three-dimensional (3D) culture systems. *Semin. Cancer. Biol.*, **2005**, *15*(5), 405-12.

[36] Abbott, A. Cell culture: biology's new dimension. *Nature*, **2003**, *424*(6951), 870-2.

[37] Miot, S.; Woodfield, T. B. F.; Daniels, A. U.; Suetterlin, R.; Peterschmitt, I.; Heberer, M.; van Blitterswijk, C. A.; Riesle, J.; Martin, I. Effects of scaffold composition and architecture on human nasal chondrocyte redifferentiation and cartilaginous matrix deposition. *Biomaterials*, **2005**, *26*(15), 2479-89.

[38] Guo, J.; Jourdian, G.; MacCallum, D. Culture and growth characteristics of chondrocytes encapsulated in alginate beads. *Connect. Tissue. Res.*, **1989**, *19*(2-4), 277-97.

[39] Tay, A. G.; Farhadi, J.; Suetterlin, R.; Pierer, G.; Heberer, M.; Martin, I. Cell yield, proliferation, and postexpansion differentiation capacity of human ear, nasal, and rib chondrocytes. *Tissue. Eng.*, **2004**, *10*(5-6), 762-70.

[40] Jakob, M.; Demarteau, O.; Schafer, D.; Hintermann, B.; Dick, W.; Heberer, M.; Martin, I. Specific growth factors during the expansion and redifferentiation of adult human articular chondrocytes enhance chondrogenesis and cartilaginous tissue formation *in vitro*. *J. Cell. Biochem.*, **2001**, *81*(2), 368-77.

[41] Xu, C.; Oyajobi, B.; Frazer, A.; Kozaci, L.; Russell, R.; Hollander, A. Effects of growth factors and interleukin-1 alpha on proteoglycan and type II collagen turnover in bovine nasal and articular chondrocyte pellet cultures. *Endocrinology*, **1996**, *137*(8), 3557-65.

[42] Yang, K. G.; Saris, D. B.; Geuze, R. E.; Helm, Y. J.; Rijen, M. H.; Verbout, A. J.; Dhert, W. J.; Creemers, L. B. Impact of expansion and redifferentiation conditions on chondrogenic capacity of cultured chondrocytes. *Tissue. Eng.*, **2006**, *12*(9), 2435-47.

[43] Benya, P. D.; Shaffer, J. D. Dedifferentiated chondrocytes reexpress the differentiated collagen phenotype when cultured in agarose gels. *Cell*, **1982**, *30*(1), 215-24.

[44] Martin, I.; Vunjak-Novakovic, G.; Yang, J.; Langer, R.; Freed, L. E. Mammalian chondrocytes expanded in the presence of fibroblast growth factor 2 maintain the ability to differentiate and regenerate three-dimensional cartilaginous tissue. *Exp. Cell. Res.*, **1999**, *253*(2), 681-8.

[45] Grigolo, B.; Lisignoli, G.; Piacentini, A.; Fiorini, M.; Gobbi, P.; Mazzotti, G.; Duca, M.; Pavesio, A.; Facchini, A. Evidence for redifferentiation of human chondrocytes grown on a hyaluronan-

based biomaterial (HYAff 11): molecular, immunohistochemical and ultrastructural analysis. *Biomaterials*, **2002**, *23*(4), 1187-95.

[46] Lu, L.; Zhu, X.; Valenzuela, R. G.; Currier, B. L.; Yaszemski, M. J. Biodegradable polymer scaffolds for cartilage tissue engineering. *Clin. Orthop.*, **2001**, *391*(Suppl), S251-70.

[47] Treppo, S.; Koepp, H.; Quan, E. C.; Cole, A. A.; Kuettner, K. E.; Grodzinsky, A. J. Comparison of biomechanical and biochemical properties of cartilage from human knee and ankle pairs. *J. Orthop. Res.*, **2000**, *18*(5), 739-48.

[48] Guilak, F.; Butler, D. L.; Goldstein, S. A. Functional tissue engineering: the role of biomechanics in articular cartilage repair. *Clin. Orthop.*, **2001**, *391*(Suppl), S295-305.

[49] Zeltinger, J.; Sherwood, J.; Graham, D.; Mueller, R.; Griffith, L. Effect of pore size and void fraction on cellular adhesion, proliferation, and matrix deposition. *Tissue. Eng.*, **2001**, *7*(5), 557-72.

[50] Baier Leach, J.; Bivens, K. A.; Patrick, C. W., Jr.; Schmidt, C. E. Photocrosslinked hyaluronic acid hydrogels: natural, biodegradable tissue engineering scaffolds. *Biotechnol. Bioeng.*, **2003**, *82*(5), 578-89.

[51] Chenite, A.; Chaput, C.; Wang, D.; Combes, C.; Buschmann, M. D.; Hoemann, C. D.; Leroux, J. C.; Atkinson, B. L.; Binette, F.; Selmani, A. Novel injectable neutral solutions of chitosan form biodegradable gels in situ. *Biomaterials*, **2000**, *21*(21), 2155-61.

[52] Cushing, M. C.; Anseth, K. S. Materials science. Hydrogel cell cultures. *Science*, **2007**, *316*(5828), 1133-4.

[53] Elisseeff, J.; Puleo, C.; Yang, F.; Sharma, B. Advances in skeletal tissue engineering with hydrogels. *Orthod. Craniofac. Res.*, **2005**, *8*(3), 150-61.

[54] Wang, D. A.; Varghese, S.; Sharma, B.; Strehin, I.; Fermanian, S.; Gorham, J.; Fairbrother, D. H.; Cascio, B.; Elisseeff, J. H. Multifunctional chondroitin sulphate for cartilage tissue-biomaterial integration. *Nat. Mater.*, **2007**, *6*(5), 385-92.

[55] Benoit, D. S.; Durney, A. R.; Anseth, K. S. The effect of heparin-functionalized PEG hydrogels on three-dimensional human mesenchymal stem cell osteogenic differentiation. *Biomaterials*, **2007**, *28*(1), 66-77.

[56] Cushing, M. C.; Liao, J. T.; Jaeggli, M. P.; Anseth, K. S. Material-based regulation of the myofibroblast phenotype. *Biomaterials*, **2007**, *28*(23), 3378-87.

[57] Gunn, J. W.; Turner, S. D.; Mann, B. K. Adhesive and mechanical properties of hydrogels influence neurite extension. *J. Biomed. Mater. Res. A*, **2005**, *72*(1), 91-7.

[58] Sharma, B.; Williams, C. G.; Kim, T. K.; Sun, D.; Malik, A.; Khan, M.; Leong, K.; Elisseeff, J. H. Designing zonal organization into tissue-engineered cartilage. *Tissue. Eng.*, **2007**, *13*(2), 405-14.

[59] Adelow, C.; Segura, T.; Hubbell, J. A.; Frey, P. The effect of enzymatically degradable poly(ethylene glycol) hydrogels on smooth muscle cell phenotype. *Biomaterials*, **2008**, *29*(3), 314-26.

[60] Patel, S.; Tsang, J.; Harbers, G. M.; Healy, K. E.; Li, S. Regulation of endothelial cell function by GRGDSP peptide grafted on interpenetrating polymers. *J. Biomed. Mater. Res. A*, **2007**, *83*(2), 423-33.

[61] Harbers, G. M.; Gamble, L. J.; Irwin, E. F.; Castner, D. G.; Healy, K. E. Development and characterization of a high-throughput system for assessing cell-surface receptor-ligand engagement. *Langmuir*, **2005**, *21*(18), 8374-84.

[62] Weber, L. M.; Hayda, K. N.; Haskins, K.; Anseth, K. S. The effects of cell-matrix interactions on encapsulated beta-cell function within hydrogels functionalized with matrix-derived adhesive peptides. *Biomaterials*, **2007**, *28*(19), 3004-11.

[63] Hwang, N. S.; Varghese, S.; Zhang, Z.; Elisseeff, J. Chondrogenic differentiation of human embryonic stem cell-derived cells in arginine-glycine-aspartate-modified hydrogels. *Tissue. Eng.*, **2006**, *12*(9), 2695-706.

[64] Lutolf, M. P.; Hubbell, J. A. Synthetic biomaterials as instructive extracellular microenvironments for morphogenesis in tissue engineering. *Nat. Biotechnol.*, **2005**, *23*(1), 47-55.

[65] Hubbell, J. A. Bioactive biomaterials. *Curr. Opin. Biotechnol.*, **1999**, *10*(2), 123-9.

[66] Hwang, N. S.; Varghese, S.; Lee, H. J.; Theprungsirikul, P.; Canver, A.; Sharma, B.; Elisseeff, J. Response of zonal chondrocytes to extracellular matrix-hydrogels. *FEBS Lett.*, **2007**, *581*(22), 4172-8.

[67] Varghese, S.; Hwang, N. S.; Canver, A. C.; Theprungsirikul, P.; Lin, D. W.; Elisseeff, J. Chondroitin sulfate based niches for chondrogenic differentiation of mesenchymal stem cells. *Matrix Biol.*, **2008**, *27*(1), 12-21.

[68] Battista, S.; Guarnieri, D.; Borselli, C.; Zeppetelli, S.; Borzacchiello, A.; Mayol, L.; Gerbasio, D.; Keene, D. R.; Ambrosio, L.; Netti, P. A. The effect of matrix composition of 3D constructs on embryonic stem cell differentiation. *Biomaterials*, **2005**, *26*(31), 6194-207.

[69] Kim, T. K.; Sharma, B.; Williams, C. G.; Ruffner, M. A.; Malik, A.; McFarland, E. G.; Elisseeff, J. H. Experimental model for cartilage tissue engineering to regenerate the zonal organization of articular cartilage. *Osteoarthritis Cartilage*, **2003**, *11*(9), 653-64.

[70] Kuo, C. K.; Ma, P. X. Ionically crosslinked alginate hydrogels as scaffolds for tissue engineering: part 1. Structure, gelation rate and mechanical properties. *Biomaterials*, **2001**, *22*(6), 511-21.

[71] Shoichet, M. S.; Li, R. H.; White, M. L.; Winn, S. R. Stability of hydrogels used in cell encapsulation: An *in vitro* comparison of alginate and agarose. *Biotechnol. Bioeng.*, **1996**, *50*(4), 374-381.

[72] Horner, H. A.; Urban, J. P. Volvo Award Winner in Basic Science Studies: Effect of nutrient supply on the viability of cells from the nucleus pulposus of the intervertebral disc. *Spine*, **2001**, *26*(23), 2543-9.

[73] Mironov, V.; Boland, T.; Trusk, T.; Forgacs, G.; Markwald, R. R. Organ printing: computer-aided jet-based 3D tissue engineering. *Trends Biotechnol.*, **2003**, *21*(4), 157-61.

[74] Smith, C. M.; Stone, A. L.; Parkhill, R. L.; Stewart, R. L.; Simpkins, M. W.; Kachurin, A. M.; Warren, W. L.; Williams, S. K. Three-dimensional bioassembly tool for generating viable tissue-engineered constructs. *Tissue. Eng.*, **2004**, *10*(9-10), 1566-76.

[75] Landers, R.; Hubner, U.; Schmelzeisen, R.; Mulhaupt, R. Rapid prototyping of scaffolds derived from thermoreversible hydrogels and tailored for applications in tissue engineering. *Biomaterials*, **2002**, *23*(23), 4437-47.

[76] Karande, T. S.; Ong, J. L.; Agrawal, C. M. Diffusion in musculoskeletal tissue engineering scaffolds: design issues related to porosity, permeability, architecture, and nutrient mixing. *Ann. Biomed. Eng.*, **2004**, *32*(12), 1728-43.

[77] Malda, J.; Woodfield, T. B. F.; van der Vloodt, F.; Kooy, F. K.; Martens, D. E.; Tramper, J.; van Blitterswijk, C. A.; Riesle, J. The effect of PEGT/PBT scaffold architecture on oxygen gradients in tissue engineered cartilaginous constructs. *Biomaterials*, **2004**, *25*(26), 5773-80.

[78] Hutmacher, D. W. Scaffolds in tissue engineering bone and cartilage. *Biomaterials*, **2000**, *21*(24), 2529-43.

[79] Wang, X. X.; Li, W.; Kumar, V. A method for solvent-free fabrication of porous polymer using solid-state foaming and ultrasound for tissue engineering applications. *Biomaterials*, **2006**, *27*(9), 1924-1929.

[80] Mikos, A.; Bao, Y.; Cima, L.; Ingber, D.; Vacanti, J.; Langer, R. Preparation of poly(glycolic acid) bonded fiber structures for cell attachment and transplantation. *J. Biomed. Mater. Res.*, **1993**, *27*(2), 183-9.

[81] Mikos, A. G.; Thorsen, A. J.; L.A., C.; Bao, Y.; Langer, R. Preparation and characterization of poly(L-lactic acid) foams. *Polymer*, **1994**, *35*, 1068-1077.

[82] Schoof, H.; Apel, J.; Heschel, I.; Rau, G. Control of pore structure and size in freeze-dried collagen sponges. *J. Biomed. Mater. Res.*, **2001**, *58*(4), 352-7.

[83] Claase, M. B.; Grijpma, D. W.; Mendes, S. C.; de Bruijn, J. D.; Feijen, J. Porous PEOT/PBT scaffolds for bone tissue engineering: Preparation, characterization, and *in vitro* bone marrow cell culturing. *J. Biomed. Mater. Res.*, **2003**, *64A*(2), 291-300.

[84] Barry, J. J.; Gidda, H. S.; Scotchford, C. A.; Howdle, S. M. Porous methacrylate scaffolds: supercritical fluid fabrication and *in vitro* chondrocyte responses. *Biomaterials*, **2004**, *25*(17), 3559-68.

[85] Zein, I.; Hutmacher, D. W.; Tan, K. C.; Teoh, S. H. Fused deposition modeling of novel scaffold architectures for tissue engineering applications. *Biomaterials*, **2002**, *23*(4), 1169-85.

[86] Wilson, C. E.; de Bruijn, J. D.; van Blitterswijk, C. A.; Verbout, A. J.; Dhert, W. J. Design and fabrication of standardized hydroxyapatite scaffolds with a defined macro-architecture by rapid prototyping for bone-tissue-engineering research. *J. Biomed. Mater. Res.*, **2004**, *68A*(1), 123-32.

[87] Leong, K. F.; Cheah, C. M.; Chua, C. K. Solid freeform fabrication of three-dimensional scaffolds for engineering replacement tissues and organs. *Biomaterials*, **2003**, *24*(13), 2363-78.

[88] Sun, W.; Lal, P. Recent development on computer aided tissue engineering - a review. *Comput. Methods. Programs. Biomed.*, **2002**, *67*(2), 85-103.

[89] Yang, S.; Leong, K.; Du, Z.; Chua, C. The design of scaffolds for use in tissue engineering. Part II. Rapid prototyping techniques. *Tissue. Eng.*, **2002**, *8*(1), 1-11.

[90] Hutmacher, D. W.; Schantz, T.; Zein, I.; Ng, K. W.; Teoh, S. H.; Tan, K. C. Mechanical properties and cell cultural response of polycaprolactone scaffolds designed and fabricated *via* fused deposition modeling. *J. Biomed. Mater. Res.*, **2001**, *55*(2), 203-16.

[91] Huang, Q.; Goh, J.; Hutmacher, D.; Lee, E. *In vivo* mesenchymal cell recruitment by a scaffold loaded with transforming growth factor beta1 and the potential for in situ chondrogenesis. *Tissue. Eng.*, **2002**, *8*(3), 469-82.

[92] Sun, W.; Starly, B.; Darling, A.; Gomez, C. Computer-aided tissue engineering: application to biomimetic modelling and design of tissue scaffolds. *Biotechnol. Appl. Biochem.*, **2004**, *39*(Pt 1), 49-58.

[93] Taboas, J.; Maddox, R.; Krebsbach, P.; Hollister, S. Indirect solid free form fabrication of local and global porous, biomimetic and composite 3D polymer-ceramic scaffolds. *Biomaterials*, **2003**, *24*(1), 181-94.

[94] Hollister, S.; Maddox, R.; Taboas, J. Optimal design and fabrication of scaffolds to mimic tissue properties and satisfy biological constraints. *Biomaterials*, **2002**, *23*(20), 4095-103.

[95] Porter, N.; Pilliar, R.; Grynpas, M. Fabrication of porous calcium polyphosphate implants by solid freeform fabrication: a study of processing parameters and *in vitro* degradation characteristics. *J. Biomed. Mater. Res.*, **2001**, *56*(4), 504-15.

[96] Hollister, S. J.; Levy, R. A.; Chu, T. M.; Halloran, J. W.; Feinberg, S. E. An image-based approach for designing and manufacturing craniofacial scaffolds. *Int. J. Oral. Maxillofac. Surg.*, **2000**, *29*(1), 67-71.

[97] Vloeberghs, M.; Hatfield, F.; Daemi, F.; Dickens, P. Soft tissue rapid prototyping in neurosurgery. *Comput. Aided. Surg.*, **1998**, *3*(2), 95-7.

[98] Woodfield, T. B. F.; van Blitterswijk, C. A.; de Wijn, J.; Sims, T. J.; Hollander, A. P.; Riesle, J. Polymer Scaffolds Fabricated with Pore-Size Gradients as a Model for Studying the Zonal Organization within Tissue-Engineered Cartilage Constructs. *Tissue. Eng.*, **2005**, *11*(9-10), 1297-1311.

[99] Malda, J.; Woodfield, T. B. F.; van der Vloodt, F.; Wilson, C.; Martens, D. E.; Tramper, J.; van Blitterswijk, C. A.; Riesle, J. The effect of PEGT/PBT scaffold architecture on the composition of tissue engineered cartilage. *Biomaterials*, **2005**, *26*(1), 63-72.

[100] Woodfield, T. B. F.; Malda, J.; de Wijn, J.; Péters, F.; Riesle, J.; van Blitterswijk, C. A., Design of porous scaffolds for cartilage tissue engineering using a three-dimensional fiber-deposition technique. *Biomaterials*, **2004**, *25*(18), 4149-4161.

[101] Habibovic, P.; Woodfield, T. B. F.; de Groot, K.; van Blitterswijk, C. A. Predictive value of *in vitro* and *in vivo* assays in bone and cartilage repair--what do they really tell us about the clinical performance? *Adv. Exp. Med. Biol.*, **2006**, *585*, 327-60.

[102] Moroni, L.; Schotel, R.; Sohier, J.; de Wijn, J. R.; van Blitterswijk, C. A. Polymer hollow fiber three-dimensional matrices with controllable cavity and shell thickness. *Biomaterials*, **2006**, *27*(35), 5918-26.

[103] Moroni, L.; Poort, G.; Van Keulen, F.; de Wijn, J. R.; van Blitterswijk, C. A. Dynamic mechanical properties of 3D fiber-deposited PEOT/PBT scaffolds: an experimental and numerical analysis. *J. Biomed. Mater. Res. A*, **2006**, *78*(3), 605-14.

[104] Moroni, L.; Hendriks, J. A.; Schotel, R.; de Wijn, J. R.; van Blitterswijk, C. A. Design of biphasic polymeric 3-dimensional fiber deposited scaffolds for cartilage tissue engineering applications. *Tissue. Eng.*, **2007**, *13*(2), 361-71.

[105] Moroni, L.; de Wijn, J. R.; van Blitterswijk, C. A. 3D fiber-deposited scaffolds for tissue engineering: influence of pores geometry and architecture on dynamic mechanical properties. *Biomaterials*, **2006**, *27*(7), 974-85.

[106] Moroni, L.; de Wijn, J. R.; van Blitterswijk, C. A. Three-dimensional fiber-deposited PEOT/PBT copolymer scaffolds for tissue engineering: influence of porosity, molecular network mesh size, and swelling in aqueous media on dynamic mechanical properties. *J. Biomed. Mater. Res. A*, **2005**, *75*(4), 957-65.

[107] Olde Riekerink, M. B.; Claase, M. B.; Engbers, G. H.; Grijpma, D. W.; Feijen, J. Gas plasma etching of PEO/PBT segmented block copolymer films. *J. Biomed. Mater. Res. A*, **2003**, *65*(4), 417-28.

[108] Mahmood, T. A.; Miot, S.; Frank, O.; Martin, I.; Riesle, J.; Langer, R.; van Blitterswijk, C. A., Modulation of chondrocyte phenotype for tissue engineering by designing the biologic-polymer carrier interface. *Biomacromolecules*, **2006**, *7*(11), 3012-8.

[109] Deschamps, A. A.; Claase, M. B.; Sleijster, W. J.; de Bruijn, J. D.; Grijpma, D. W.; Feijen, J. Design of segmented poly(ether ester) materials and structures for the tissue engineering of bone. *J. Controll. Release*, **2002**, *78*(1-3), 175-86.

[110] Bezemer, J. M.; Grijpma, D. W.; Dijkstra, P. J.; van Blitterswijk, C. A.; Feijen, J. A controlled release system for proteins based on poly(ether ester) block-copolymers: polymer network characterization. *J. Controll. Release*, **1999**, *62*(3), 393-405.

[111] van Dijkhuizen-Radersma, R.; Peters, F. L.; Stienstra, N. A.; Grijpma, D. W.; Feijen, J.; de Groot, K.; Bezemer, J. M. Control of vitamin B12 release from poly(ethylene glycol)/poly(butylene terephthalate) multiblock copolymers. *Biomaterials*, **2002**, *23*(6), 1527-36.

[112] van Blitterswijk, C. A.; van den Brink, J.; Leenders, H.; Bakker, D. The effect of PEO ratio on degradation, calcification and bone-bonding of PEO/PBT copolymer (Polyactive). *Cells Mater.*, **1993**, *3*(23), 23-36.

[113] Radder, A. M.; Leenders, H.; van Blitterswijk, C. A. Interface reactions to PEO/PBT copolymers (Polyactive) after implantation in cortical bone. *J. Biomed. Mater. Res.*, **1994**, *28*(2), 141-51.

[114] Beumer, G. J.; van Blitterswijk, C. A.; Bakker, D.; Ponec, M. Cell-seeding and *in vitro* biocompatibility evaluation of polymeric matrices of PEO/PBT copolymers and PLLA. *Biomaterials*, **1993**, *14*(8), 598-604.

[115] Claase, M. B.; Olde Riekerink, M. B.; de Bruijn, J. D.; Grijpma, D. W.; Engbers, G. H.; Feijen, J. Enhanced bone marrow stromal cell adhesion and growth on segmented poly(ether ester)s based on poly(ethylene oxide) and poly(butylene terephthalate). *Biomacromolecules*, **2003**, *4*(1), 57-63.

[116] Beumer, G. J.; van Blitterswijk, C. A.; Ponec, M. Biocompatibility of a biodegradable matrix used as a skin substitute: an *in vivo* evaluation. *J. Biomed. Mater. Res.*, **1994**, *28*(5), 545-52.

[117] Li, P.; Bakker, D.; van Blitterswijk, C. A. The bone-bonding polymer Polyactive 80/20 induces hydroxycarbonate apatite formation *in vitro*. *J. Biomed. Mater. Res.*, **1997**, *34*(1), 79-86.

[118] Sakkers, R. J.; Dalmeyer, R. A.; de Wijn, J. R.; van Blitterswijk, C. A. Use of bone-bonding hydrogel copolymers in bone: an *in vitro* and *in vivo* study of expanding PEO-PBT copolymers in goat femora. *J. Biomed. Mater. Res.*, **2000**, *49*(3), 312-8.

[119] Mendes, S. C.; Bezemer, J.; Claase, M. B.; Grijpma, D. W.; Bellia, G.; Degli-Innocenti, F.; Reis, R. L.; de Groot, K.; van Blitterswijk, C. A.; de Bruijn, J. D. Evaluation of two biodegradable polymeric systems as substrates for bone tissue engineering. *Tissue. Eng.*, **2003**, *9*(Suppl 1), S91-101.

[120] Wang, H. J.; Bertrand-De Haas, M.; Van Blitterswijk, C. A.; Lamme, E. N. Engineering of a dermal equivalent: seeding and culturing fibroblasts in PEGT/PBT copolymer scaffolds. *Tissue. Eng.*, **2003**, *9*(5), 909-17.

[121] Woodfield, T. B. F.; Miot, S.; Martin, I.; van Blitterswijk, C. A.; Riesle, J. The regulation of expanded human nasal chondrocyte re-differentiation capacity by substrate composition and gas plasma surface modification. *Biomaterials*, **2006**, *27*(7), 1043-53.

[122] Mahmood, T. A.; de Jong, R.; Riesle, J.; Langer, R.; van Blitterswijk, C. A. Adhesion-mediated signal transduction in human articular chondrocytes: the influence of biomaterial chemistry and tenascin-C. *Exp. Cell. Res.*, **2004**, *301*(2), 179-88.

[123] Moroni, L.; Licht, R.; de Boer, J.; de Wijn, J. R.; van Blitterswijk, C. A. Fiber diameter and texture of electrospun PEOT/PBT scaffolds influence human mesenchymal stem cell proliferation and morphology, and the release of incorporated compounds. *Biomaterials*, **2006**, *27*(28), 4911-22.

[124] Bezemer, J. M.; Oude Weme, P.; Grijpma, D. W.; Dijkstra, P. J.; van Blitterswijk, C. A.; Feijen, J. Amphiphilic poly(ether ester amide) multiblock copolymers as biodegradable matrices for the controlled release of proteins. *J. Biomed. Mater. Res.*, **2000**, *52*(1), 8-17.

[125] Zanetti, N. C.; Solursh, M. Effect of cell shape on cartilage differentiation. In *Cell shape: determinants, regulation and regulatory role*, Stein, W. D.; Bronner, F., Eds.; Academic Press: New York, **1989**, pp. 291-327.

[126] Odgaard, A. Three-dimensional methods for quantification of cancellous bone architecture. *Bone*, **1997**, *20*(4), 315-28.

[127] Muschler, G. F.; Nakamoto, C.; Griffith, L. G. Engineering principles of clinical cell-based tissue engineering. *J. Bone. Joint. Surg. Am.*, **2004**, *86-A*(7), 1541-58.

[128] Radisic, M.; Malda, J.; Epping, E.; Geng, W.; Langer, R.; Vunjak-Novakovic, G. Oxygen gradients correlate with cell density and cell viability in engineered cardiac tissue. *Biotechnol. Bioeng.*, **2006**, *93*(2), 332-43.

[129] Malda, J.; Rouwkema, J.; Martens, D. E.; Le Comte, E. P.; Kooy, F. K.; Tramper, J.; van Blitterswijk, C. A.; Riesle, J. Oxygen gradients in tissue-engineered PEGT/PBT cartilaginous constructs: Measurement and modeling. *Biotechnol. Bioeng.*, **2004**, *86*(1), 9-18.

[130] Lewis, M. C.; MacArthur, B. D.; Malda, J.; Pettet, G.; Please, C. P. Heterogeneous proliferation within engineered cartilaginous tissue: The role of oxygen tension. *Biotechnol. Bioeng.*, **2005**, *91*(5), 607-615.

[131] Kellner, K.; Liebsch, G.; Klimant, I.; Wolfbeis, O.; Blunk, T.; Schulz, M.; Gopferich, A., Determination of oxygen gradients in engineered tissue using a fluorescent sensor. *Biotechnol. Bioeng.*, **2002**, *80*(1), 73-83.

[132] Obradovic, B.; Meldon, J.; Freed, L.; Vunjak-Novakovic, G. Glycosaminoglycan deposition in engineered cartilage: Experiments and mathematical model. *AIChE J.*, **2000**, *46*, 1860-1871.

[133] Sengers, B. G.; van Donkelaar, C. C.; Oomens, C. W.; Baaijens, F. P. Computational study of culture conditions and nutrient supply in cartilage tissue engineering. *Biotechnol. Prog.*, **2005**, *21*(4), 1252-61.

[134] Freed, L. E.; Marquis, J. C.; Vunjaknovakovic, G.; Emmanual, J.; Langer, R. Composition of Cell-Polymer Cartilage Implants. *Biotechnol. Bioeng.*, **1994**, *43*(7), 605-614.

[135] Pettet, G. J.; Please, C. P.; Tindall, M. J.; McElwain, D. L. The migration of cells in multicell tumor spheroids. *Bull. Math. Biol.*, **2001**, *63*(2), 231-57.

[136] Hollister, S. J., Porous scaffold design for tissue engineering. *Nat. Mater.*, **2005**, *4*(7), 518-24.

[137] Gratson, G. M.; Xu, M.; Lewis, J. A. Microperiodic structures: direct writing of three-dimensional webs. *Nature*, **2004**, *428*(6981), 386.

[138] Lin, C. Y.; Kikuchi, N.; Hollister, S. J. A novel method for biomaterial scaffold internal architecture design to match bone elastic properties with desired porosity. *J. Biomech.*, **2004**, *37*(5), 623-36.

[139] Stevens, M. M.; George, J. H. Exploring and engineering the cell surface interface. *Science*, **2005**, *310*(5751), 1135-8.

[140] Badami, A. S.; Kreke, M. R.; Thompson, M. S.; Riffle, J. S.; Goldstein, A. S. Effect of fiber diameter on spreading, proliferation, and differentiation of osteoblastic cells on electrospun poly(lactic acid) substrates. *Biomaterials*, **2006**, *27*(4), 596-606.

[141] Li, W. J.; Jiang, Y. J.; Tuan, R. S. Chondrocyte phenotype in engineered fibrous matrix is regulated by fiber size. *Tissue. Eng.*, **2006**, *12*(7), 1775-85.

[142] Schantz, J. T.; Hutmacher, D. W.; Lam, C. X.; Brinkmann, M.; Wong, K. M.; Lim, T. C.; Chou, N.; Guldberg, R. E.; Teoh, S. H. Repair of calvarial defects with customised tissue-engineered bone grafts II. Evaluation of cellular efficiency and efficacy *in vivo*. *Tissue. Eng.*, **2003**, *9*(Suppl 1), S127-39.

[143] Schantz, J. T.; Teoh, S. H.; Lim, T. C.; Endres, M.; Lam, C. X.; Hutmacher, D. W. Repair of calvarial defects with customized tissue-engineered bone grafts I. Evaluation of osteogenesis in a three-dimensional culture system. *Tissue. Eng.*, **2003**, *9*(Suppl 1), S113-26.

[144] Adachi, T.; Osako, Y.; Tanaka, M.; Hojo, M.; Hollister, S. J. Framework for optimal design of porous scaffold microstructure by computational simulation of bone regeneration. *Biomaterials*, **2006**, *27*(21), 3964-72.

[145] Hollister, S.; Lin, C.; Saito, E.; Schek, R.; Taboas, J.; Williams, J.; Partee, B.; Flanagan, C.; Diggs, A.; Wilke, E.; Van Lenthe, G.; Muller, R.; Wirtz, T.; Das, S.; Feinberg, S.; Krebsbach, P. Engineering craniofacial scaffolds. *Orthod. Craniofac. Res.*, **2005**, *8*(3), 162-73.

[146] Lin, C. Y.; Schek, R. M.; Mistry, A. S.; Shi, X.; Mikos, A. G.; Krebsbach, P. H.; Hollister, S. J. Functional bone engineering using ex vivo gene therapy and topology-optimized, biodegradable polymer composite scaffolds. *Tissue. Eng.*, **2005**, *11*(9-10), 1589-98.

[147] Hollister, S. J.; Lin, C. Y.; Schek, R. D.; Taboas, J. M.; Flanagan, C. L.; Saito, E.; Williams, J. M.; Das, S.; Wirtz, T.; Krebsbach, P. H. Design and fabrication of scaffolds for anatomic bone reconstruction. *Med. J. Malaysia.*, **2004**, *59*(Suppl B), 131-2.

[148] Lin, C. Y.; Hsiao, C. C.; Chen, P. Q.; Hollister, S. J. Interbody fusion cage design using integrated global layout and local microstructure topology optimization. *Spine*, **2004**, *29*16), 1747-54.

[149] Starly, B.; Yildirim, E.; Sun, W. A tracer metric numerical model for predicting tortuosity factors in three-dimensional porous tissue scaffolds. *Comput. Methods. Programs.. Biomed.*, **2007**, *87*(1), 21-7.

[150] O'Brien, F. J.; Harley, B. A.; Waller, M. A.; Yannas, I. V.; Gibson, L. J.; Prendergast, P. J. The effect of pore size on permeability and cell attachment in collagen scaffolds for tissue engineering. *Technol. Health Care*, **2007**, *15*(1), 3-17.

Received: September 28, 2007 **Revised: December 12, 2007** **Accepted: June 6, 2008**